DISSERTATIONES SCHOLAE DOCTORALIS AD SANITATEM INVESTIGANDAM
UNIVERSITATIS HELSINKIENSIS

EMMI PALOMÄKI

NEW INSIGHTS INTO CRYSTALLIZATION OF AMORPHOUS MATERIALS

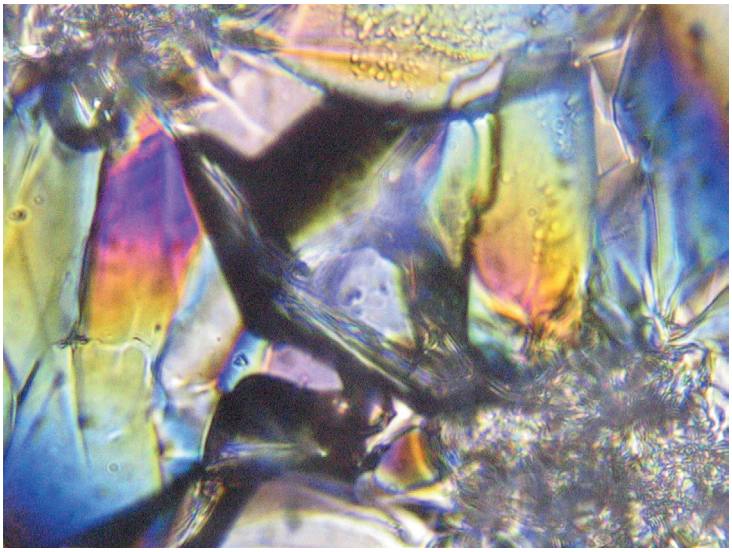

DIVISION OF PHARMACEUTICAL CHEMISTRY AND TECHNOLOGY
FACULTY OF PHARMACY
DOCTORAL PROGRAMME IN DRUG RESEARCH
UNIVERSITY OF HELSINKI

Division of Pharmaceutical Chemistry and Technology
Faculty of Pharmacy
University of Helsinki
Finland

NEW INSIGHTS INTO CRYSTALLIZATION OF AMORPHOUS MATERIALS

Emmi A. K. Palomäki

DOCTORAL DISSERTATION

To be presented for public discussion with the permission of the Faculty of Pharmacy of the University of Helsinki, in Auditorium 1041, Biocenter 2 (Viikinkaari 5), on 16th of October 2020 at 12 o'clock.

Helsinki 2020

Supervisors Prof. Emer. Jouko Yliruusi
Division of Pharmaceutical Chemistry and Technology
Faculty of Pharmacy
University of Helsinki
Finland

Prof. Clare Strachan
Division of Pharmaceutical Chemistry and Technology
Faculty of Pharmacy
University of Helsinki
Finland

Docent Henrik Ehlers
Division of Pharmaceutical Chemistry and Technology
Faculty of Pharmacy
University of Helsinki
Finland

Tiina Lipiäinen, Ph.D.
Research Scientist
R&D, Global Pharmaceutical Research
Inhalation Product Development
Orion Corporation
Finland

Reviewers Docent Satu Lakio
Pharmaceutical Development Manager
Nanoform Finland Ltd
Finland

Assoc. Prof. Andrea Heinz
LEO Foundation Center for Cutaneous Drug Delivery
Department of Pharmacy
University of Copenhagen
Denmark

Custos Prof. Jouni Hirvonen
Division of Pharmaceutical Chemistry and Technology
Faculty of Pharmacy
University of Helsinki
Finland

Opponent Docent Jari Pajander
Principal Scientist
Late Formulation & Process Development
LEO Pharma
Denmark

Dissertationes Scholae Doctoralis Ad Sanitatem Investigandam Universitatis Helsinkiensis

ISBN 978-951-51-6410-0 (pbk.)
ISBN 978-951-51-6411-7 (PDF)

Hansaprint
Helsinki 2020

ABSTRACT

Palomäki E.A.K., 2020. **New insights into crystallization of amorphous materials**

Dissertationes Scholae Doctoralis Ad Sanitatem Investigandam Universitatis Helsinkiensis, 56/2020, pp. 54
ISBN 978-951-51-6410-0 (Paperback)
ISBN 978-951-51-6411-7 (PDF, http://ethesis.helsinki.fi)
ISSN 2342-3161 (Print)
ISSN 2342-317X (Online)

Drugs must dissolve upon administration to have a therapeutic effect. Nowadays, most new drug candidates are poorly water-soluble, which makes this solubility issue a significant global challenge. Solubilization can be enhanced using formulation-based solutions, particle size reduction, salt formation, prodrugs or amorphization of the drug. This thesis concerns the last approach, amorphization. Unlike highly ordered crystalline materials, amorphous materials lack long range order. This leads to amorphous materials having greater molecular mobility and free energy, and consequently solubility, than their crystalline counterparts. However, the solubility benefits of the amorphous form come with a price, since the thermodynamic instability of amorphous materials means they tend to crystallize.

Pharmaceutical products need to be sufficiently physically and chemically stable throughout their entire shelf life to ensure their efficacy and safety. In the case of amorphous drugs, there are still many aspects about crystallization that are not fully understood. The aim of the thesis was to investigate factors influencing the crystallization process in single and multiphase amorphous systems, as well as complexities in monitoring the progression of crystallization.

The crystallization of several one- and two-phase amorphous systems were investigated, with the influence of both excipients and atmospheric gas on the crystallization process being investigated. Raman spectroscopy and X-ray diffractometry were used to monitor crystallization in the study, and their sensitivities and suitability to measure crystallization in the samples of interest were considered. Differential scanning calorimetry (DSC), Fourier transform infrared spectroscopy (FTIR) and optical microscopy were used to provide complementary information on crystallization processes.

In the present thesis it was found that excipients and atmospheric gases that interact with amorphous material, even in the absence of mixing and specific interactions, can delay the onset of crystallization. Additionally, it was found that Raman spectroscopy is not necessarily suitable for crystallinity

determination, when the opacity of the sample changes, as can happen at temperatures above T_g.

Overall, this thesis demonstrates that several factors, beyond those usually considered in traditional single-phase solid dispersions, can influence crystallization, and that these, together with the effect of measurement technique artefacts, should be carefully considered when developing amorphous formulations.

ACKNOWLEDGEMENTS

This work was mainly carried out in the Division of Pharmaceutical Chemistry and Technology, Faculty of Pharmacy, University of Helsinki, Finland, during the years of 2013-2020. Part of the measurements in Article I were done in the Physics department, Faculty of Science, University of Helsinki. I gratefully acknowledge all the funding sources that made the work possible, including the Academy of Finland (Suomen Akatemia), the Orion Research Foundation sr, the Vilho, Yrjö and Kalle Väisälä Foundation and the University of Helsinki Funds.

I want to express my great gratitude towards my supervisor, Professor Emeritus Jouko Yliruusi. You inspired me already in the first days of my studies at the university by being so passionate about the philosophy of science. Our collaboration began when I started my Master's thesis project and continued during my PhD project. I would not be here without you believing in me, giving me the chance to work in your project and being such a good science excitement catalyst! Thank you!

I want to express my great gratitude towards my supervisor, Professor Clare Strachan. Thank you for all the great discussions during the writing of the 3rd article of the thesis and the thesis itself. Thank you for your great scientific input, language checks and emotional support!

I want to express my great gratitude towards my supervisor, docent Henrik Ehlers. While you still worked at the university, you were always there for me, whenever I wanted to share scientific problems or exciting results with someone. You were a super active supervisor, who was always positive and ready to discuss science. After you left university, you still continued to supervise me and gave your great scientific input. Thank you!

I want to express my great gratitude towards my supervisor, PhD Tiina Lipiäinen. Thank you for your scientific input, your friendship and all the encouragement!

I want to thank our collaborators at the Physics department at the University of Helsinki. PhD Patrik Ahvenainen, University Lecturer Kirsi Svedström, Professor Simo Huotari and the late Professor Ritva Serimaa. I want to thank you all for always making me feel welcome. Additionally, I want to thank you for your scientific input on my thesis.

Next, I want to thank all the other great people (all not mentioned by name) at the University of Helsinki who have helped me during the years.

I want to thank our laboratory engineer, PhD Heikki Räikkönen for your time and effort you have used to help me whenever I needed to build something for my projects. Additionally, I want to thank you for all the support, encouragement and great scientific discussions.

I want to thank Markus Selin for all the scientific discussions and all the support you have given me during my bachelor's and master's studies, as well as during my PhD studies.

PhD Dunja Novakovic, thank you for being such a warm and supportive friend, who is always ready to listen and discuss. You have lightened up my PhD journey a lot! Thank you!

PhD Jukka Saarinen, thank you for being such a great travel mate on conference trips. Thank you for all the discussions and all support during my PhD studies.

Jaana Koskela and PhD Jenni Pessi are thanked for being friends who are always ready to discuss and give support.

It's time to thank people outside the university, who have helped me during my doctoral studies, but also earlier, when I built the base for my future. Thank you all!

I want to thank you, my dear friend Sanna, for the lovely friendship we have. Over 30 years ago (Sic!), we started to play together. At an age when children are usually not able to play together (but rather side by side), we did! Today, you are still one of my best friends. We might not see every week or month, but our bond is unbreakable. Thank you for being the brave one! You have taught me that even though I might be scared, I can still be brave. Without you, I would be many experiences poorer. Thank you for all the love and support you have given me during all these years!

I want to thank you, my dear friend Tiina. Thank you for all the great discussions. You have helped me through rough times and always supported me. Thank you!

I want to thank you, my dear friend Miina. Thank you for great discussions, for broadening my views and all the relaxed nights you have spent with me. Thank you for all the love and support you have given me!

I want to thank you, my dear friend Lauri. Thank you for all the countless good discussions we have had. Thank you for the game nights and long walks. Thank you for being such a supportive and loving friend, who is always willing to talk and give new perspectives!

I want to thank you, my dear friend Sari. We found each other on the entrance exam day and again when we started our studies at the Faculty of Pharmacy. Thank you for your friendship, all the support, great game nights and all the great discussions!

I want to thank my dear handicraft-friends, Anni-Helena and Oona. You found your way to my heart way faster than people usually do. You have been a part of my life when I have grown most as a human. I sincerely think that you have been important, positive factors on my growth. Thank you for sharing all the good times and all the bad times! Thank you for all the love and support!

Additionally, I want to thank my board game friends, Eurovision friends and bouldering friends. Also, all other friends that have helped me get through these years are thanked.

I want to thank my "vice mother" Leena and "vice father" Markku. Even though we are not family, you are like second parents to me. Thank you for all the support you have given me during the years. Thank you, Leena, for saving my life as a toddler and always being there for me. Thank you, Markku, for teaching me that sometimes the only difference between ordinary and super is the mindset. It has been a privilege to have you in my life. Thank you!

I want to thank my family and relatives for always supporting and loving me. My mum Virpi and dad Esko are thanked for all the support and encouragement you have given me during my life. Mum and dad, most of all I appreciate your unconditional love and you always encouraging me to find my own path – whatever it is. Thank you! I want to thank my little brother, Ismo. As a child, you were a good fighting buddy – nowadays, you are good friend of mine. Thank you for your love, support and great discussions as well as great board game nights. My little brother, Timo, is thanked for the love, support and new perspectives. Already as a young child, you forced me to think about little nuances of life and made me question how much I actually knew. You are still doing the same thing, which I highly appreciate.

Finally, my warmest thanks to Perttu, my love. Thank you for all the love and support you have given me. You have helped me lift myself up when I have been at the bottom. You have made every moment of success and happiness way more amazing. Your endless acceptance and kindness of your heart make my soul sing. With you, even mathematics doesn't follow the rules it used to. With you 1+1>>2.

Helsinki, July 2020

Emmi Palomäki

A highly organized poem

In our universe,
chaos always increases.
One always resists;
wanting to become ordered.
Amorphous material!

-Emmi Palomäki

CONTENTS

LIST OF ORIGINAL PUBLICATIONS

This thesis is based on the following publications:

I Palomäki E., Ahvenainen P., Ehlers H., Svedström K., Huotari S., Yliruusi J., Monitoring the recrystallization of amorphous xylitol using Raman spectroscopy and wide-angle X-ray scattering. *International Journal of Pharmaceutics* 508, 71-82, 2016.

II Palomäki E.A.K., Yliruusi J.K., Ehlers H.V., Effect of headspace gas on nucleation of amorphous paracetamol. *Journal of Drug Delivery Science and Technology* 51, 127-138, 2019.

III Palomäki E.A.K., Lipiäinen T., Strachan C.J., Yliruusi J.K., 2020. Effect of trehalose and melibiose on crystallization of amorphous paracetamol. Submitted manuscript.

The publications are referred to by their Roman numerals. Papers are reprinted with the kind permission of Elsevier.

ADDITIONAL PUBLICATION

Additional publication, which is not included in the experimental part of this thesis:

1. Palomäki E., Ehlers H., Antikainen O., Sandler N., Yliruusi J., Non-destructive properties of microcrystalline cellulose compacts. *International Journal of Pharmaceutics*. 2015, 495(2), 633-641.

ABBREVIATIONS

API	Active pharmaceutical ingredient
ATR	Attenuated total reflectance
CESS	Controlled Expansion of Supercritical Solutions
CLS	Classical least squares analysis
CO_2	Carbon dioxide
DSC	Differential scanning calorimetry
DVS	Dynamic vapor sorption
e.g.	*exempli gratia*, for example
FT-ATR-IR	Fourier transform attenuated total reflectance infrared spectroscopy
FTIR	Fourier transform infrared spectroscopy
GI tract	Gastrointestinal tract
i.e.	*id est*, in other words
ILS	Inverse least squares analysis
IMC	Isothermal microcalorimetry
IR	Infrared
MLR	Multiple linear regression
m/m	Mass/mass
MSC	Multiplicative scatter correction
MTDSC	Modulated temperature differential scanning calorimetry
N_2	Nitrogen
NA	Not applicable
NIR	Near-infrared
O_2	Oxygen
PC	Principal component
PCA	Principal component analysis
PCR	Principal components regression
PET	Polyethylene terephthalate
Ph. Eur.	European Pharmacopoeia
PLM	Polarized light microscopy
PLS	Partial least squares
PXRD	Powder X-ray diffraction
Q^2	Predictability (of the model)
R^2	Goodness (of the model)
RESS	Rapid expansion of supercritical solution
RH%	Relative humidity-%
SAXS	Small-angle X-ray scattering
SC	Solution calorimetry
SCXRD	Single crystal X-ray diffraction
SEM	Scanning electron microscopy

SNV	Standard normal variate
ss-NMR	Solid-state nuclear magnetic resonance
T_g	Glass transition temperature
TGA	Thermogravimetric analysis
T_m	Melting temperature/melting point
TPS	Terahertz pulsed spectroscopy
WAXS	Wide-angle X-ray scattering
XRPD	X-ray powder diffraction

1 INTRODUCTION

When a patient takes a medicine orally for systemic delivery, the active pharmaceutical ingredient (API) must be dissolved to have a therapeutic effect. Adequate solubility of the API guarantees fast enough dissolution and a sufficient dissolved drug concentration in the gastrointestinal tract (GI tract). Even the most potent drug molecule is rendered useless, if it does not get to the target site, which usually would require the API to be dissolved first.

An increasing amount of new drug molecule candidates are large in size and include functional groups which render them poorly water-soluble (Cooper, 2010; Lipinski, 2002). This is a remarkable global challenge. However, there are approaches to make the API more soluble. In addition to formulation-based solutions, the API can be made to dissolve faster, for example through salt or prodrug formation, reducing particle size or rendering the material in an amorphous form (Hancock and Zografi, 1997; Laitinen et al., 2013; Mu et al., 2013; Serajuddin, 1999; Vasconcelos et al., 2007; Yu, 2001). Amorphous material is disordered, with a greater free energy and molecular movement than in crystalline forms (Laitinen et al., 2013). Amorphous forms are thus significantly more water-soluble than crystalline forms. On the other hand, they are physically unstable and tend to crystallize (Bhugra and Pikal, 2008).

Pharmaceuticals need to be manufactured in a way that ensures the quality criteria to be met through the shelf life of the product. If chemical or physical stability fails, the drug product might lose its therapeutic effect or have a different effect than anticipated. Consequently, crystallization of amorphous materials needs to be better understood and controlled to enable amorphous drugs to be used more commonly and ensure safe and effective medical treatments.

The overall aim of this thesis was to obtain new information on factors influencing the measurement and process of crystallization of amorphous materials.

2 REVIEW OF THE LITERATURE

2.1 AMORPHOUSNESS AND POLYMORPHISM

Typically, solid materials composed of small molecules are in a crystalline form, i.e. they have long range molecular order. Many materials have multiple polymorphic forms. Indomethacin, for example, has at least seven polymorphic forms (Surwase et al., 2013), whereas xylitol has only been documented to have one stable form and one metastable form (Wolfrom and Kohn 1942; Carson et al., 1943). If no energy is added to the system, crystallization of an amorphous material is an irreversible process.

Amorphous solids have the highest free energy of solid forms while different polymorphic forms have lower but varying levels of free energy, depending on their crystalline structure (Fig. 1). Solid materials tend to convert towards their lowest energy forms, which leads to crystallization of amorphous materials and polymorphic conversions between different polymorphs. This difference in potential energy levels for polymorphs is caused by the differences in molecular packing (Cui, 2007). Amorphous materials and different polymorphic forms have a significant role in pharmaceutics because of their different solubilities, as well as other differences e.g. in mechanical properties, packing properties, thermodynamic properties, kinetic properties and surface properties (Grant, 1999).

Figure 1. A schematic representation of different forms of a substance with the same chemical composition. A) crystalline stable form I, b) crystalline metastable form II and c) unstable amorphous form. The letter e represents a single molecule. Crystal defects in crystalline materials have been illustrated using grey color.

When crystalline material is liquefied, for example by heating above its melting point (T_m), molecules have higher mobility compared to in the solid crystalline state, where they are restricted within a certain ordered structure by directional intermolecular forces (Goldstein, 1968). When the liquid is cooled fast enough, molecules do not have enough time to rearrange and form long range order (crystallize) (Cui, 2007). Instead, a disordered amorphous solid is formed, in which there is no long-range molecular order (Cui, 2007). Depending on the amorphized compound, preparation method and storage condition, the amorphous system can remain unchanged from only seconds to

years (Cui, 2007). Since many pharmaceutical amorphous APIs tend to crystallize in a time scale that is too short for them to be used in a pure amorphous API form, the tendency to crystallize needs to be altered. Stabilization of amorphous materials is discussed in section 2.5.

An important characteristic of any amorphous material is its glass transition temperature (T_g). At temperatures lower than T_g, the amorphous material is in the glassy state, and at temperatures higher than the T_g, it is in the rubbery state. A key difference between those states is that in the glassy state, the crystallization is less likely and slower below T_g, compared to above the T_g (Craig et al., 1999). This is linked to the material having a higher viscosity and molecular mobility at lower temperatures.

2.2 METHODS FOR PREPARING AMORPHOUS MATERIAL

There are multiple ways to generate amorphous materials. Methods commonly used on the industrial scale are freeze-drying (Lai and Topp, 1999; Wang 2000), spray-drying (Beyerinck et al., 2003a, 2003b), spray-freezing (Yu et al., 2006) and melt extrusion (Sprockel et al., 1997). Some other methods for preparing amorphous materials are cooling or quench cooling of melt, milling and grinding (Patterson et al., 2005), dehydration of hydrated crystals (Li et al., 2000), high pressure compaction (Smith and Gauzer, 2003) and electric field application (Weinhold et al., 1984). Other methods involving liquid (including a solution) as a starting material are antisolvent addition (Guillory, 1999), pH change (Guillory, 1999), vacuum systems (Szoke et al., 2005; Abdul-Fattah et al., 2008), rapid expansion of supercritical solution (RESS) (Ye and Wai, 2003) and controlled expansion of supercritical solutions (CESS) (Pessi et al., 2016). Further methods with solid or liquid as a starting material are electrospinning (Igantious and Sun, 2005) and ultrasound (Suslick and Price, 1999; Ruecroft et al., 2005). All of them have their benefits and drawbacks.

In the laboratory (on a small scale), amorphous pharmaceutical solids can often be made by cooling melted material either fast or slowly. Traditionally, it has been thought that amorphous materials need to be cooled rapidly to restrict molecular rearrangement during cooling and thus obtain the non-ordered rubbery or glassy amorphous form. However, in some cases amorphous pharmaceutical solid might be more stable after slow cooling than fast cooling (Martínez et al., 2014; Willart et al., 2017). The reason for that can be, for example, cracks formed during fast cooling, which can lead to nucleation and subsequent crystallization (Martínez et al., 2014; Willart et al., 2017).

2.3 PHARMACEUTICAL RELEVANCE OF THE AMORPHOUS FORM

An increasing proportion of new pharmaceutical drug candidates are poorly water-soluble. Amorphous materials may have solubilities 10 – 1600 times higher than those of their stable crystalline counterparts (Hancock and Parks, 2000), which makes amorphization an attractive option.

Low water-solubility is not only a challenge in a therapeutic sense, but also a great financial problem. Fewer new drug candidates are identified annually and an increasing proportion of the new candidates are usable in their most stable polymorphic form. Increasing knowledge about the amorphous form and crystallization is, consequently, highly valuable also from the financial perspective.

In addition of different solubility of the amorphous form compared to polymorphs, amorphous form can have different mechanical properties, processability and chemical stability.

2.4 FACTORS INFLUENCING CRYSTALLIZATION OF AMORPHOUS MATERIALS

To ensure sufficient physical stability of amorphous material for pharmaceutical use, the influence of aspects intrinsic to the amorphous material itself, as well as environmental conditions, on crystallization must be understood. In this section, these aspects are presented.

2.4.1 BEGINNING OF CRYSTALLIZATION

Crystallization is two-step process, where first stable nuclei form and subsequently nuclei grow rapidly. There are many factors influencing crystallization initiation, such as molecular mobility and hydrogen bonding (Liu et al., 2006; Yu, 2001). If there are many hydrogen donors and acceptors in the molecule, they can form many relatively strong hydrogen bonds between the molecules in the amorphous form (Bhende and Jadhav, 2012). This can lead to a situation where the material is less likely to form ordered groups of molecules (Bhende and Jadhav, 2012). Consequently, stable nuclei are not easily formed. Additionally, molecules need to overcome possible steric hindrance, which prevents molecules from having contacts between suitable functional groups and consequently form stable nuclei (Ovshinsky, 1985).

There are two types of crystallization – homogeneous and heterogeneous. Çelikbilek et al. (2012) have summarized the difference: “The nucleation either occurs without the involvement of a foreign substance in the interior of the parent phase, which is called “homogeneous or primary nucleation” or with the contact of the parent phase with a foreign substance that acts as a preferred nucleation site which is called “heterogeneous or secondary nucleation”. A

factor causing heterogeneous nucleation can be for example container walls (Çelikbilek et al., 2012), impurities (Viel et al., 2017) and excipients (Bhatt et al., 2015; Martínez et al., 2014; Hellrup and Mahlin, 2011). Also cracks can cause heterogeneous nucleation by greatly increasing the surface area in contact with the gas phase (Patterson et al., 2005; Dudognon et al., 2008). If heterogeneous nucleation is possible, it is usually favored, since it requires less free energy than homogeneous nucleation (Turnbull, 1950).

2.4.2 DIFFERENT CRYSTALLIZATION TENDENCIES OF DIFFERENT MATERIALS

Small inflexible molecules tend to crystallize easier than large flexible molecules. In addition to more pronounced steric hindrance effects, bigger molecules have more degrees of freedom with respect to their molecular conformation, as well as possible hydrogen bonding interactions, which can complicate formation of crystal structure (Almarsson and Gardner, 2003; Almarsson and Zaworotko, 2004).

While the most suitable amorphized materials for pharmaceutical development are those that do not crystallize easily, rapidly crystallizing materials are useful for general research into crystallization behavior, including external factors that can affect crystallization. Rapidly crystallizing systems can provide new information on crystallization without taking years – or decades. Thus, it is beneficial to investigate systems that crystallize fast and later on investigate systems that crystallize slower.

2.4.3 SEED PARTICLES

When amorphous material is manufactured by grinding, it is likely to contain some seed crystals of some polymorph of the original crystalline material (Sandhu et al., 2014). These seed crystals may act as nuclei to start crystal growth. Residual crystallinity or the presence of any crystalline material in the amorphous material, regardless of the manufacturing process used, can be a problem, especially when the nucleation step during crystallization is circumvented.

2.4.4 FOREIGN SURFACES

When amorphous material is in contact with a foreign surface, the presence of the foreign surface can lead to crystallization (Hellrup and Mahlin, 2011; Bhatt et al., 2015). Such surfaces can be interfaces between amorphous material and gaseous phase (Byrn et al., 2001; Chen et al. 2002), container (Martínez et al., 2014) or other material in two-phase or multiple-phase systems (Yu et al., 1998). Two- or multiple-phase systems include controlled and uncontrolled impurities. However, in some cases additives can also lead to stabilization of

the amorphous system as discussed in section 2.5. Having cracks in the system makes the solid-gas interface much bigger, which leads to crystallization being more likely (Martínez et al., 2014; Willart et al., 2017).

2.4.5 WATER

When two materials with different T_gs are mixed on a molecular level, they can attain one T_g (Hancock and Zografi 1994). Since water has a T_g of -135°C (Haque and Roos, 2003), it can lower the T_g of amorphous material significantly, especially, since amorphous materials tend to adsorb more water than crystalline materials. As an example, it has been reported that when water content of amorphous xylitol is 0%, its T_g is -24°C (Talja and Roos, 2001). The T_g is -53°C when the water content is 10% and -93°C when the water content is 40%. When the T_g decreases below storage temperature, amorphous materials become rubbery (Yu, 2016). The lower viscosity is associated with increased molecular mobility. Consequently, diffusion of molecules in the bulk increases, leading to an increased crystallization rate.

2.4.6 OTHER ATMOSPHERIC GASES

There has been a lack of systematic research into the effect of atmospheric gases other than water on the crystallization of amorphous materials. The lack of research is somewhat surprising, since the interactions between molecules in solid and gaseous phases are known to take place and water is known to have a significant impact on the stability of amorphous materials. As stated earlier in the thesis (2.4.1), hydrogen bonds play a very important role in crystallization. If the gas can interact with the functional groups that would otherwise form hydrogen bonds with other molecules in the amorphous material, gas may have an effect on crystallization.

Amorphous materials are known to interact more freely with atmospheric water than their crystalline counterparts. Also other gases have been reported to act similarly. According to Byrn et al. (2001) amorphous DL-Ala-DL-Met-dipeptide oxidized to a significantly higher extent than its crystalline counterpart. This indicates that amorphous material interacted more with oxygen than its crystalline counterpart, which is likely due to the amorphous materials having higher free volume, greater molecular mobility and more possibility for forming new bonds. Di Martino et al. (2000) reported that when subjecting amorphous indomethacin or crystalline α-indomethacin to gaseous ammonia, indomethacin chemically reacted with the gas. However, crystalline γ-indomethacin did not react with the gas. The study showed that interaction with the gaseous phase requires an exposed reactive functional group.

2.4.7 TEMPERATURE

Some molecular movement is needed for nuclei to form. Nucleation is fastest near the T_g (Craig et al., 1999). However, between T_g and T_m the nucleation rate decreases, when the movement of molecules increases. However, since the crystal growth is faster at higher temperatures, the overall-crystallization can increase, when the temperature increases.

The glassy state (temperature below T_g) is more physically stable than the supercooled state (temperature above T_g), but in both cases crystallization may occur, although it is more likely in temperatures above T_g (Ediger et al., 1996). It has been said that to guarantee stability, amorphous materials should be stored at a temperature that is at least 50°C lower than T_g. However, for some materials this temperature difference is not sufficient, since it has been reported that crystallization might occur even 175°C below T_g (Okamoto and Oguni, 1996). Additionally, one must remember that humidity lowers the T_g, which can also have a major impact on finding suitable storage conditions for amorphous materials.

2.4.8 PROCESS-INDUCED CRYSTALLIZATION

When amorphous material is processed, it may be exposed to conditions that may cause it to crystallize. Roughly, process-induced crystallization can be divided into water-induced crystallization, heat-induced and pressure induced crystallization. Some processes can be in multiple categories.

After preparation of amorphous material, milling can be needed to make formulation of the material possible. Milling can lead to a rise in temperature (Morales et al., 2012), which makes crystallization of the material more likely (Craig et al., 1999; Ediger et al., 1996). Additionally, shear forces introduce a large amount of energy to the system (Merisko-Liversidge et al., 2003), which can have an effect on crystallization. Other processes used during the manufacturing of the drug product that expose the material to heat are granulation (Sandhu et al., 2014) and tableting (DeCrosta et al., 2001). In tableting, the material is exposed to high pressure, which can lead to crystallization of amorphous materials (Lakio et al., 2015). Granulation can also expose the material to a solvent, often water (Sandhu et al., 2014). In the coating process, amorphous material can be exposed to water as well as heat (Sandhu et al., 2014; Sauer et al., 2013).

2.4.9 CRYSTALLIZATION DURING DISSOLUTION

Considering the outcome of medical treatment, it is not sufficient to have an amorphous system that remains stable through the shelf-life of the product. The amorphous form needs to withstand the conditions it is subjected to upon administration. It is known that amorphous systems may recrystallize when in

contact with aqueous media, whereby the stability advantage is lost and the active ingredient is rendered ineffective (Alonzo et al., 2010). In the GI tract, the drug environment changes drastically. It faces highly acidic and less acidic aqueous conditions. The rough and changing conditions may lead to amorphous drug crystallizing, which may lead it to losing the enhanced solubility properties, which can restrict dissolution rate to be the same or even lower than it would have with stable crystalline form.

2.5 STABILIZATION OF THE AMORPHOUS FORM

Protecting amorphous material from elevated humidity and temperature is not always enough to guarantee stability of the amorphous form long enough time for therapeutic use. Consequently, stabilizing agents often need to be added to ensure the amorphous drug remains stable. These agents can be for example polymers, sugars, amino acids or porous materials. In this section, sugars and porous materials are described more in depth.

To get two or more materials to form a stable amorphous system, they need to have sufficiently strong molecular interactions to prevent similar molecules from forming bonds and starting to form nuclei (Bughra and Pikal, 2008). Optimally, the materials are miscible and can be mixed on a molecular level to form one homogeneous phase (Brough and Williams, 2013). However, also two-phase systems can prevent crystallization (Semjonov et al., 2017).

In the stabilization of small molecules in an amorphous form, commonly used group of excipients is polymers (Asmus et al., 2012; Baghel et al., 2016; Vaka et al., 2014). Due to their long chains, they can form a wide network, which prevents amorphous small molecules moving freely, which prevents crystallization (Baghel et al., 2016; Vaka et al., 2014).

Usage of non-ordered mesoporous silica and other porous materials is based on their ability to absorb small drug molecules into the pores and interact with drug molecules, preventing them from crystallizing (Kinnari et al., 2011; Limnell et al., 2011). In earlier studies, silica (Syloid 244 FP) has been loaded with drug using immersion (Kinnari et al., 2011; Limnell et al., 2011), rota-evaporation (Limnell et al., 2011) and fluid bed processing (Limnell et al., 2011). With such loading, the molecules cannot get in contact with each other in large enough quantities to be able to form stable nuclei and/or support crystal growth.

Sugars are typically used in the stabilization of amorphous protein formulations (Davidson and Sun, 2001; Lipiäinen et al., 2016, 2018). They can immobilize the protein molecules, and inhibit unfolding as well as aggregation (Izutsu et al., 1993; Mensink et al., 2013). Small molecule excipients have been found more efficient in protein stabilization than larger molecules, since small molecules have a better ability to form direct bonds with proteins compared to larger molecules (Mensink et al., 2017; Tonnis et al., 2015).

In addition to protein stabilization, small molecules, such as amino acids and sugars, can be used to stabilize other small molecules. In some cases, two small molecules can form a co-amorphous system, which can prevent crystallization effectively (Chavan et al., 2016; Gao et al., 2013; Löbmann et al., 2013a, 2013b, 2013c). In other cases, they can form two-phase systems, in which crystallization is prevented or postponed (Brough and Williams, 2013; Semjonov et al., 2017).

2.6 INVESTIGATING CRYSTALLINITY AND POLYMORPHISM

There are many techniques that can be used when characterizing amorphous pharmaceuticals and different polymorphs (Chieng et al., 2011).

Spectroscopic measurements that probe materials on the molecular level include:

- Raman spectroscopy
- Mid-IR, including Fourier transform infrared (FTIR) spectroscopy
- Near infrared (NIR)
- Solid-state nuclear magnetic resonance (ss-NMR).

Measurement techniques that probe the particulate level include:

- Terahertz pulsed spectroscopy (TPS),
- X-ray methods including single crystal X-ray diffraction (SCXRD), small-angle X-ray scattering (SAXS) and wide-angle X-ray scattering (WAXS), which in pharmaceutical studies, is often referred as powder X-ray diffraction (PXRD or XRPD)
- Thermoanalytical and gravimetric analyses, including differential scanning calorimetry (DSC), modulated temperature differential scanning calorimetry (MTDSC), thermogravimetric analysis (TGA), dynamic vapor sorption (DVS), isothermal microcalorimetry (IMC) and solution calorimetry (SC)
- Microscopy, including polarized light microscopy (PLM), with or without a hot/cryo/freeze-drying stage, and scanning electron microscopy (SEM).

From these, WAXS (**I-III**), DSC (**I-III**) and PLM (**I-II**) are presented in more detail in this section. Additionally, data analysis is discussed in this section.

2.6.1 X-RAY DIFFRACTION

X-ray diffraction crystallography is the primary method used when studying crystallinity, crystallite size or polymorphism of pharmaceutical compounds. It is based on scattering of X-rays caused by the electron clouds of individual atoms in the sample. Based on data collected from variations of the intensity

of scattered x-rays, information on atomic packing, interatomic forces and angles can be obtained (Dong and Boyd 2011). Unknown materials cannot be identified using x-ray diffraction, since the method does not provide information on chemical composition (Chieng et al., 2011). However, polymorphic forms of known substances can be identified. When studying amorphous systems, x-ray scattering is an indirect method, which does not provide direct structure information on disorder, but rather on the lack of order.

2.6.2 DIFFERENTIAL SCANNING CALORIMETRY (DSC)

Differential scanning calorimetry (DSC) is a method that provides quantitative information about endothermic reactions (such as melting) and exothermic reactions (such as crystallization) as a function of time and temperature (Clas et al., 1999). Also heat capacity changes (such as glass transition) can be investigated. Detecting the glass transition enables detection of amorphousness, and detecting the melting peak can enable determination of the polymorphic form of the investigated material (Clas et al., 1999). The effect of water on the T_g may be observed (Talja and Roos, 2001). Impurities may be detected (van Dooren and B.W. Müller, 1984; Giron and Goldbronn, 1993). All of these can help to further understand the results of other measurements.

2.6.3 SPECTROSCOPIC MEASUREMENTS

2.6.3.1 Fourier transform infrared (FTIR) spectroscopy

Infrared (IR) spectroscopy is a method that is based on energy absorption associated with vibrations of atoms in molecules (Berthomieu and Hienerwadel, 2009; Blum and John, 2012). The introduction of Fourier transform spectrometers has dramatically improved the quality of data due to the much better signal-to-noise ratio (Blum and John, 2012). For the molecule to be detectable with IR a change in dipole moment is needed, which typically happens with asymmetric vibrations of polar functional groups (Berthomieu and Hienerwadel, 2009). It can be used to differentiate polymorphs and amorphous samples and to quantify crystallinity (Akao et al., 2001; Amado et al., 2017). Additionally, it can be determined whether or not a mixture has molecular interactions between the components, in particular hydrogen bonding (Crupi et al., 2007; Löbmann et al., 2013c).

2.6.3.2 Raman spectroscopy

Raman spectroscopy is based on inelastic scattering of monochromatic (laser) light caused by molecular vibrations associated with a change in polarizability (as opposed to a change in dipole moment for FTIR) (Colthup et al., 1990; Larkin, 2011). As a result, a small portion of the incident light is scattered at slightly longer wavelengths (Stokes scattering) or even more rarely at shorter wavelengths (anti-Stokes-scattering). Stokes and anti-Stokes scattering are collectively known as Raman scattering. Raman spectroscopy is best in detecting symmetric vibrations of non-polar groups, and is relatively insensitive to water (Larkin, 2011). When using Raman spectroscopy, fluorescence can be a big problem. Typically, it can be seen as an elevated and curved baseline in the measured Raman spectra of the sample (Pelletier,2003). However, when measuring highly fluorescent samples, such as colored samples, the Raman response can be completely masked by the fluorescence (Pelletier,2003; McCreery, 2000). This interference can be at least partially avoided by, for example, using a longer laser wavelength that is less likely to induce fluorescence (e.g. 785 nm instead of 532 nm). When IR and Raman sample preparation are compared, Raman measurements are generally simpler. With Raman spectroscopy the sample does not need to be in contact with the probe and/or diluted.

2.6.3.3 Spectral pretreatments and multivariate analysis

In many cases, when multiple spectra are involved and differences between the spectra are of interest, the spectral data need to be pretreated and processed using multivariate analysis. There can be variations in intensity and changes in baseline, which could be caused by differences in particle size, density, sample packing and fluorescence (Pellow-Jarman et al., 1996; Savolainen et al., 2006). Additionally, in the vibrational (e.g. Raman) spectra interpretation can be complicated by overlapping peaks and subtle changes that can be impossible to detect visibly (Heinz et al., 2009; Aaltonen et al., 2008). Combined these do not enable e.g. comparison of peak intensities or areas. A combination of suitable pretreatment and multivariate methods is valuable for both qualitative and quantitative spectral interpretation and can make results more reliable.

The effect of baseline differences can be overcome using baseline correction or derivatives. To remove overall spectral intensity differences, for example, standard normal variate (SNV) or multiplicative scatter correction (MSC) can be used. Usage of carefully selected spectral pre-treatments can make multivariate analysis more reliable (Savolainen et al., 2006). They are compared in detail in section 5.1.2.

The most common multivariate analysis methods for spectral data in pharmaceutical sciences have been divided into two categories: classical least

squares analysis (CLS) and inverse least squares analysis (ILS) approaches (Strachan et al., 2007). CLS is recommended to be used when all components of the sample are known. It can be divided to direct and indirect CLS. ILS approaches are recommended to be used, when not all components are known. Common ILS methods are multiple linear regression (MLR), principal components regression (PCR, principal component analysis (PCA) combined with linear regression) and partial least squares (PLS).

2.6.4 OPTICAL MICROSCOPY

Optical microscopy can be used to visually examine samples and confirm findings from other techniques. It is an additional method that can be used to visually examine the difference in crystallite size and polymorphism based on the crystal habit (Greco and Bogner, 2010). When polarized light is used, amorphous and crystalline areas of the sample can be differentiated, since, between cross polarizers, birefringent crystals rotate the plan of the polarized light and appear brightly colored, while isotropic amorphous particles do not and appear dull/black (Kestur and Taylor, 2013; Wu et al., 2007).

3 AIMS OF THE STUDY

The overall aims of this thesis were to obtain new insights into the crystallization of non-traditional two-phase amorphous systems and the effect of the gaseous phase on the crystallization of amorphous material. Furthermore, the thesis set out to bring new insights into the characterization of crystallization of these systems.

The specific objectives were:

- to investigate effect of analytical technique and data processing method on quantification of crystallization of rapidly recrystallizing systems at temperatures above T_g (**I**)
- to investigate how atmospheric gases affect the onset of crystallization of amorphous API (**II**)
- to study the effect of excipients on crystallization of two-phase amorphous solid dispersions (**I, III**).

4 EXPERIMENTAL

4.1 MATERIALS (I-III)

Several model substances were used in the crystallization studies **I-III**. The starting materials were crystalline xylitol (University Pharmacy, Finland) (**I**) and crystalline paracetamol form I (Orion Pharma, Finland) (**II-III**). To alter crystallization of these substances, non-ordered mesoporous silica (Syloid 244 FP, Grace GmbH & Co., KG, Germany) (**I**), D-(+)-trehalose dihydrate (Sigma, USA) (**III**) and D-melibiose monohydrate (Senn Chemicals, Switzerland) (**III**) were used. Additionally, ibuprofen (Boots Pharmaceuticals, United Kindom) (**I**) and γ-indomethacin (Orion Pharma, Finland) were used in the Raman spectroscopy penetration depth studies (**I**).

Xylitol and non-ordered mesoporous silica were kept over silica gel in a desiccator for at least two weeks prior to the experiments to minimize water content (**I**). In article **II**, the paracetamol samples were kept in a glove box with set atmospheres of humid air, dry air, dry carbon dioxide (CO_2) or dry nitrogen (N_2) at least 10 minutes in equilibrium humidity before the melting process.

Xylitol (**I**) is a small sugar alcohol, which is often used as a sweetener. It has a molar mass of 152.1 g/mol. Amorphous xylitol has a very low T_g of -24°C (Talja and Roos, 2001) and only one stable polymorphic form and one metastable form are known (Carson et al., 1943; Diogo et al., 2007). These factors make xylitol a good model compound for investigating rapid recrystallization.

Non-ordered mesoporous silica (**I**) is a material composed of particles with nanosized pores, which can be loaded with drug molecules. In the case of Syloid 244 FP, the particle size is 2.5 – 3.7 μm and the pore volume is 1.6 ml/g (Grace GmbH & Co., 2015). Depending on the pore size, surface area and surface chemistry, the material can be suitable for stabilizing different drugs in the amorphous form (Xu et al., 2013). In this study, non-ordered mesoporous silica (also referred to in the thesis as silica) is used to alter the crystallization rate of amorphous xylitol. In this study, mixing was performed using the melting. The ratio of silica to API in this study was less than in most previous studies, where aim has been to the fill pores and have no free API. In this case, a lower proportion of silica was used, to allow higher drug loadings and simultaneously allow the effects of simple mixing on crystallization and its measurement to be investigated.

Paracetamol (**II-III**) is a non-steroidal analgesic drug. It was selected based on it being representative of typical organic drugs having an aromatic polyfunctional structure. It has a molecular weight of 151.2 g/mol. Paracetamol has three polymorphs, of which form I is the stable form (Perrin et al., 2009). It has a T_g in the region of 22 – 26°C (Qi et al., 2008).

Trehalose (**III**) and melibiose (**III**) are disaccharides with a molecular mass of 342.3 g/mol. There is a wide range of T_gs reported for trehalose, with values varying between 100 and 120°C, but most listed are in the range of 115 – 120°C (Hancock and Dalton, 1999; Hancock and Zografi, 1997; Heljo et al., 2012; Kadoya et al., 2010; Quo et al., 1999; Roos, 1993; Surana et al., 2004; Sussich et al., 1998). Melibiose has been reported to have T_gs of 85°C (Roos, 1993), but also 100°C (Heljo et al., 2012). Trehalose is widely used in protein stabilization, with melibiose having been studied to a lesser degree. Heljo et al. (2012) and Lipiäinen et al. (2016, 2018) have compared these disaccharides in protein stabilization. However, these disaccharides have not been compared in stabilizing small molecules, even though trehalose has been successfully used in small molecule stabilization earlier (Mazzobre et al., 2003; Horvat et al., 2005; Luthra et al., 2008).

4.2 METHODS (I-III)

4.2.1 SAMPLE PREPARATION (I-III)

In all cases, amorphous samples were prepared using melting and cooling (**I-III**). This sample preparation section is arranged according to measurement technique, with more specific sample preparation details mentioned where appropriate within these subsections.

4.2.1.1 Wide-angle x-ray scattering (WAXS) and Raman spectroscopy samples (I-III)

In article **I**, the whole sample preparation process from melting to closing the sample holder was done in a glove box with a dry nitrogen atmosphere. A sample size of 1.35 g was used, since the amount could fill the sample holder. The sample holder enabled *in situ* analysis with both X-ray and Raman measurements and kept the atmosphere similar between measurements. Amorphous xylitol was prepared by melting crystalline xylitol powder on a hot plate at 180°C, which is well above the melting point of xylitol (92 – 96°C). This ensured proper mixing with silica and was well below the boiling point of xylitol (215 – 217°C). Non-ordered mesoporous silica 10% (m/m) was mixed into the molten xylitol. The mixture of molten xylitol and silica was quench-cooled and ground roughly in liquid nitrogen. When most of the liquid nitrogen had evaporated, the sample was poured into the sample holder with left over liquid nitrogen. When the liquid nitrogen had totally evaporated, the sample was sealed in the sample holder between two plastic films. The plastic films were 6 μm thick Mylar films made from the resin polyethylene terephthalate (PET). This was done to ensure a repeatable dry nitrogen atmosphere inside the sample holder. The final samples had a diameter of 15

mm and a thickness of 2 mm. WAXS and Raman measurements were initiated 4 min after complete liquid nitrogen evaporation.

For crystallinity quantification based on Raman spectroscopic data, reference samples of xylitol with crystalline contents of 0% (n=5), 10% (n=3), 25% (n=3), 40% (n=3), 50% (n=5), 60% (n=3), 75% (n=3), 90% (n=3) and 100% (n=5) were prepared. The amorphous fraction of the sample was prepared as described above. A known amount of crystalline xylitol was added to the xylitol-liquid nitrogen dispersion and gently ground to create the mixture. Since silica gave a negligible Raman response, a second reference set with silica was not prepared.

With the WAXS measurements, the quantitative model was based on diffractograms of the average of the first three minutes of the amorphous xylitol measurement, crystalline xylitol and non-ordered mesoporous silica. The xylitol crystallinity values were then calculated from the areas under the sample intensity curve of xylitol and the amorphous contribution. The xylitol crystallinity values were normalized with the average crystallinity value of the crystalline xylitol measurement.

In article **II**, the whole sample preparation process from melting to closing the sample holder was done in a glove box with set atmospheres of dry air with a relative humidity of 4.4 – 4.7%, nitrogen (N_2) with a relative humidity of 0.0 – 0.1%, carbon dioxide (CO_2) with a relative humidity of 1.2 – 1.5% or humid air with a relative humidity of 21.1 – 22.2%. The gases were conducted into the glove box using a pressure of 1.6 bar. In this study, 10.00 ± 0.08 mg of crystalline paracetamol was placed on the sample holder and melted on a hot plate for 3.5 – 4 min. The temperature was set to 210°C, but, due to heat loss, the sample reached a temperature of approximately 190°C. The sample was cooled down to the temperature prevalent in the glove box (15.55 ± 0.45°C) using a metal block with a temperature of 13.15 ± 0.25°C. The sample holder was closed containing the selected atmosphere, whereby the sample was ready for Raman measurements. The first measurement point was 10 min after cooling in all experiments. Reference samples of amorphous paracetamol, and crystalline paracetamol forms I and II were made according to Kauffman et al. (2008). These reference samples were made in triplicate. To determine if PCA could be directly used in crystallinity determination, reference samples with varying crystallinities consisting of amorphous and form II of paracetamol were prepared.

In article **III**, 1.00 g of sample containing 25%(m/m) of paracetamol and 75%(m/m) of sugar (melibiose or trehalose) was spread in the aluminum pan to increase the contact area and reduce melting time as much as possible. The sample was mixed during melting using a spatula to get sample as homogeneously mixed as possible. Melting temperatures were 195°C for paracetamol, melibiose and paracetamol-melibiose samples and 215°C for trehalose and paracetamol-trehalose samples to ensure complete melting of the sample. Heating was continued 20 sec after appearing completely molten to ensure that the sample was fully melted and thus amorphous. Longer

melting times exposed the sample to chemical degradation, which could be seen as color changes. Cooling was performed in a glove box with nitrogen atmosphere by pouring liquid nitrogen into the pan. In 4 s, the sample had reached the temperature of liquid nitrogen. Residual liquid nitrogen was poured out of the pan after 1 min. The sample was transferred into a mortar, ground, transferred to the sample holder and sealed in the sample holder. The sample holder had a set volume and plastic films (Mylar) on top and below the sample. The final sample sizes were 151 ± 8 mg. Preparation was followed by WAXS measurements.

In all articles (**I-III**), samples showing any sign of possible degradation (as evidenced by a color change) were discarded from the crystallization behavior analyses. In crystallization studies **I-II**, the samples were not moved during the continuous measurements. In article **III**, the sample was stored at 38 ± 0.5°C and 75 ± 1% and 3 ± 1% relative humidities between measurements.

4.2.1.2 Differential scanning calorimetry (DSC) samples (I-III)

All DSC samples were prepared in 40 µl aluminum pans and the pans were covered with pinhole lids to allow humidity evaporation. Amorphous samples in the sample holder (**II**) were made similarly as the Raman spectroscopy samples, but the sample was detached from the microscope slide and transferred to the DSC pan. Other samples (**I-III**) were taken from bulk or from ground material, and measured as such. Samples were weighed using an analytical balance.

4.2.1.3 Fourier transform infrared (FTIR) samples (III)

Samples for FTIR analysis were produced the same way as for WAXS analysis. However, amorphous paracetamol reference samples were not ground, since it crystallized so rapidly that grinding would have caused it to crystallize before measurement.

4.2.1.4 Optical microscopy samples (I-II)

Separate amorphous xylitol and amorphous xylitol-silica dispersions (**I**) were produced in a similar manner to that described above in section 4.2.1.1. Samples were set as thin layers on microscope slides. Additional samples were made by placing some of the final products on microscope slides, molten and quench cooled by dipping the sample to liquid nitrogen.

In article **II**, paracetamol samples were prepared in a dry nitrogen atmosphere in a similar manner as for the Raman spectroscopy samples described above in section 4.2.1.1.

4.2.2 MEASUREMENTS

In this section, the technical aspects of all analytical methods used in this thesis are presented. WAXS and Raman spectroscopy were used to monitor crystallization. WAXS measurements were done in transmission mode, so that the whole sample was equally represented, whereas with Raman spectroscopy, the measurements were based on back scattering, which meant that the upper region in the sample (closer to the sampling probe) was over-represented. DSC was used to measure T_g, recrystallization and T_m, which could give more information on possible differences of the T_g, which could explain possible shifts in onsets of crystallization and changes in recrystallization rates. Additionally, DSC was used in determining polymorphic forms of the end products. Optical microscopy was used to visually observe how crystallization progressed and evaluate the crystallite sizes present in the end products. FTIR spectroscopy was used to detect possible interactions between components of the solid dispersions.

4.2.2.1 Wide-angle X-ray scattering (WAXS) (I-III)

In article **I**, WAXS measurements were performed using a Rigaku rotating-anode based X-ray set-up (Kontro et al., 2014) with a Pilatus 1M detector. The beam size was 1 mm^2. Measurement times were 5 or 15 s and measurements were conducted continuously. These diffractograms were averaged over 60 s and corrected as described in Dixon et al. (2015). Overall measurement times were 15 min for crystalline xylitol reference, 90 min for amorphous xylitol and 150 min for the xylitol-silica dispersion. Amorphous xylitol reference was combined from the diffractograms of first 3 min of the amorphous xylitol measurement. The measurements were performed at ambient conditions: 19.2 – 31.3% relative humidity and 28.7 – 29.3°C temperature (detected outside the sample holder).

In articles **II-III**, WAXS measurements were performed using an Empyrean X-Ray diffractometer (Panalytical, Almelo, Netherlands). A fixed divergence slit of 0.19 mm, general voltage of 45 kV and tube current of 40 mA were used.

In article **II**, the step size was 0.01313°, the measured angular range was 5 – 50° and the overall measurement time was 24.45 min. Measurements were conducted in reflection mode. The resulting polymorphic forms of the selected samples were measured from samples that were exposed to atmospheric gases of dry air, humid air or nitrogen and the highest and lowest temperatures were investigated. The purpose of the WAXS measurements was to confirm that the samples had converted to the polymorphic form indicated in the Raman spectra.

In article **III**, the step size was 0.01313°, the measured angular range was 5 – 25° and the overall measurement time was 6.2 min. A narrower angular range was selected to make measurement faster and consequently minimize sample exposure to lower temperatures of 25 – 27°C. A 10 mm x 10 mm area

was measured using Parabolic Mirror transmission. The sample holder was kept closed during the measurement and open while stored at the temperature of 38 ± 0.5°C and relative humidity of 75 ± 1%. Those conditions are within the limits of elevated temperature and humidity conditions set for stability studies. Crystallization observations of 1:3 solid dispersions of amorphized paracetamol-trehalose and paracetamol-melibiose were done in triplicate.

4.2.2.2 Differential scanning calorimetry (DSC) (I-III)

All DSC samples were measured using differential scanning calorimetry (DSC; DSC823e, Mettler-Toledo Inc., Switzerland). In every measurement the heating rate was 10°C/min.

In article **I**, bulk xylitol and non-ordered mesoporous silica, as well as examples of freshly prepared quench-cooled samples and examples of crystalline end products were analyzed. The samples were cooled to -50°C, heated to 0°C, re-cooled to -50°C and heated up to 140°C.

In article **II**, bulk paracetamol, representative samples of freshly prepared amorphous materials and end products that were kept at 18.3°C or 28.3°C were measured. Samples were held at -20°C for 5 min and heated to 200°C.

In article **III**, reference samples, amorphous samples of paracetamol, trehalose and melibiose and physical mixtures of paracetamol-trehalose and paracetamol-melibiose were measured. Additionally, each batch used in WAXS measurements was analyzed immediately after preparation and after crystallization. All samples were kept at 10°C for 5 min, heated to 100°C, cooled to 0°C and heated up to 250°C.

4.2.2.3 Fourier transform infrared spectroscopy (FTIR) (III)

FTIR analyses were done using a single-reflection MIRacle attenuated total reflectance (ATR) crystal (Pike Technologies, Wisconsin, USA) and a Vertex 70 spectrometer (Bruker Optics, Ettlingen, Germany). Data was collected using OPUS 5.5 (Bruker Optics, Ettlingen, Germany) software. Each spectrum was the average of 256 scans and the spectral resolution was 4 cm^{-1}. The used spectral range was 1400–1800 cm^{-1}.

4.2.2.4 Raman spectroscopy (I-II)

All Raman spectroscopy measurements (**I-II**) were done using a Raman RXN1-PhAT-785-D spectrometer (Kaiser, USA) and a PhAt system probe head (Kaiser optical systems, Inc., USA). The laser source had a laser power of 400-mW and a wavelength of 785 nm (Raman RXN1-PhAT-785-D, Kaiser optical systems, Inc., USA). The spectral resolution was 0.3 cm^{-1} and Raman shifts between 200 cm^{-1} and 1800 cm^{-1} were used. The beam diameter was 6 mm, which is relatively large. A larger beam diameter minimizes the spectrometer's

sensitivity to inhomogeneities of sample and the exact positioning of the sample (Johansson et al., 2005; Paudel et al., 2015). Additionally, when the effect of laser power is spread over a larger area, the heat load becomes smaller. In all measurements, one result was the average of three scans. In article **I**, the measurement integration time was 2 s. In article **II**, the integration time was 0.5 s.

In article **I**, two different recrystallization measurement sets were investigated. In the first measurement set, the relative humidity was 21 – 35% and the temperature was between 20.1 – 21.6°C. The recrystallization process was observed for 6 hours with 1-min intervals. In the second measurement set, recrystallization was performed at an elevated temperature of 28.5 – 29.5°C and relative humidity of 19 – 25%. These conditions corresponded to the conditions in the WAXS measurements. Measurements were performed at 5-min intervals until the sample was fully crystalline. These crystallization experiments were done in triplicate. Every reference sample was done in triplicate, except the 0%, 50% and 100% samples, which were done as five separate samples.

In article **II**, the Raman measurements were performed through the bottom of the sample. In the re-crystallization experiments, spectra were collected at 30-sec intervals. Measurement sets were performed at four temperatures: well below onset of T_g (17.2 ± 0.3°C), slightly below onset of T_g (21.7 ± 0.2°C), slightly above onset of T_g (23.9 ± 0.4°C) and well above onset of T_g (27.5 ± 0.2°C). The reference samples were measured three times each.

4.2.2.5 Optical microscopy (I-II)

In articles **I-II**, a polarizing light microscope (Nikon Optishot; Tokyo, Japan) was used. Measurements were performed at ambient conditions (**I**) or in a N_2 atmosphere and 20.5 – 21.4°C temperature (**II**).

4.2.3 DATA ANALYSIS

In this section, the pretreatment and data analysis performed on the WAXS and Raman spectroscopy results are presented.

4.2.3.1 Crystallinity analysis of WAXS samples

In article **I**, reference samples of bulk xylitol and non-ordered mesoporous silica were used to assess the contribution of xylitol and silica in solid dispersions using least-squares fitting. Based on the WAXS results, in the measured area, the sample was composed of 13% of silica. This amount was expected to be constant during measurements and the silica contribution to the diffractogram was subtracted from all the data points of xylitol-silica

dispersion, which led to data representing only xylitol. Crystallinity values were obtained from the amorphous xylitol scattering patterns and the sharp diffraction peaks. Crystallinity values of xylitol were calculated from the areas under the sample intensity curve and amorphous contribution.

In article **II**, X-ray diffractometry was used to confirm the polymorphic form of paracetamol after crystallization monitoring with Raman spectroscopy. Paracetamol polymorph identification was done by visual inspection of the diffractograms.

In article **III**, there were two crystallizing materials in each sample. Therefore, the method to determine crystallinity described earlier in this section could not be used. The crystallinities of paracetamol, melibiose and trehalose samples were determined using selected peak heights from the X-ray diffractograms. Before height determination, HighScore Plus (Malvern Panalytical Ltd, Malvern, United Kingdom) was used to subtract the baseline from the input data. In the software, the sending factor was set to 30 and granulatory to 40. Peak positions were determined using minima of the 2nd derivatives and the peak heights were determined in the same software.

A sample-mass-based correction factor was used to ensure as accurate crystallinity determination as possible. The selected peaks (2θ) were at 9.8° for crystalline melibiose, at 14.6° for crystalline trehalose and at 18.2° for crystalline paracetamol. Calibration samples for the quantitative model were done in triplicate and contained crystalline paracetamol and excipient in fractions of 0, 25, 50, 75 and 100%. R^2-values for the linear fittings (set intercept to 0) were 0.948 for paracetamol, 0.806 for trehalose and 0.934 for melibiose. The lower R^2-values for the trehalose model were assumed to be caused by the overlapping shoulder of another peak.

4.2.3.2 Partial least squares (PLS) (I)

Since the Raman peaks of amorphous and crystalline xylitol are overlapping, PLS regression was used to analyze the Raman spectra. The Raman shift range (835.2 – 1145.4 cm^{-1}) used in the PLS model was selected to ensure most of the strong and moderate characteristic peaks were included (de Veij et al., 2009). These peaks include the in-phase ν(CCO) stretching vibration at 872 cm^{-1} and the peaks in the 1000 – 1150 cm^{-1} range, representing the out-of-phase δ(CCO) stretching vibration. Additionally, the range was only mildly affected by fluorescence.

Extensive investigation to reveal and the select the best combination of pretreatments was performed prior to PLS modelling. Pretreatments contained baseline correction, mean centering, Savitzky-Golay 1st and 2nd derivatives, standard normal variate (SNV) and multiplicative scatter correction (MSC). MATLAB (MatLab R2014b, MathWorks Inc., Natick, Massachusetts, United States) was used for all spectral pretreatments, except MSC, which was done using SimcaP 10.5 (Umetrics AB, Umeå, Sweden). The baseline correction was done with Matlab function msbackadj (windowsize 25,

stepsize 25). The selection of the best combination of pretreatments is presented in section 5.2.

4.2.3.3 Principal component analysis (PCA) (II)

To identify which polymorphic form of paracetamol crystallized, three reference samples of amorphous paracetamol, paracetamol form I and paracetamol form II were prepared using the method described by Kauffman et al. (2008). Form III could not be prepared, because the sample holder did not allow a method where it could have formed. Spectra were pretreated with Savitzky-Golay smoothing (window size 9, 3rd degree equation) and 1st derivative transformation. PCA was used to analyze the spectral range of 1586.7 – 1686.3 cm^{-1}. The spectral range was selected because it includes two characteristic peaks, which reveal the polymorphic form of paracetamol (Nanubolu et and Burley, 2012; Kauffman et al., 2008).

After determining that all samples crystallized to form II, reference samples containing known amounts of form II and the amorphous form were prepared. Spectra were analyzed with PCA and the first principal component (PC1) was plotted against the reference crystallinity values. There was linear correlation between PC1 and crystallinity, which enabled direct use of PC1 values in determining the crystallinity of paracetamol samples at different time points.

5 RESULTS AND DISCUSSION

5.1 CHALLENGES IN CRYSTALLINITY DETECTION (I)

In this section, the first objective of the thesis is addressed. Raman spectroscopy and WAXS are compared as methods to monitor crystallization in temperatures above T_g. Additionally, the effects of spectral data pretreatments on crystallinity quantification were investigated.

5.1.1 DIFFERENCES BETWEEN RESULTS IN CRYSTALLINITY DETERMINATION USING RAMAN SPECTROSCOPY AND WAXS

In this section, Raman spectroscopy and WAXS are compared as methods for crystallinity determination at temperatures above T_g. There have been many studies comparing spectroscopic techniques and X-ray diffraction to characterize crystallization below T_g, but studies above T_g are lacking. Priemel et al. (2012) reported that x-ray suggested slower crystallization than Fourier transform attenuated total reflectance infrared spectroscopy (FT-ATR-IR) spectroscopy below T_g. This was due to crystallization being fastest at the particle surfaces. FT-ATR-IR measures only the surface of the sample (approximately 1-2 μm sampling depth), whereas X-ray analysis samples entire particles or even samples (in conventional diffraction setups).

Mah et al. (2014) reported that during milling crystalline glibenclamide became x-ray amorphous, when it was still partly crystalline based on Raman spectroscopy. To conclude, Raman spectroscopy was found to be more sensitive in detecting small amounts of crystallinity from the amorphous samples compared to x-ray. In this case, the difference was attributed to Raman spectroscopy being more sensitive to shorter-range order than X-ray diffraction analysis.

These studies illustrate that several measurement factors, including sampling depth and different sensitivities to length scales of order, can affect quantitative crystallinity measurement, and this section further investigates measurement effects, including in samples above T_g.

Raman spectroscopy is typically considered a surface biased or sensitive technique when probing solid pharmaceutical materials due to strong elastic scattering the laser light employed and tightly focused laser beams leading to relatively small spot sizes. However, in this study the Raman spectrometer setup used involved collimated (unfocused) laser light which increases the sampling volume, allowing measurements much deeper into the sample. Additionally, the beam size is relatively large with a diameter of 6 mm, which guarantees good sample representation.

In the present study, when crystallization of pure amorphous xylitol was detected with Raman spectroscopy at a temperature of 20.1-21.6°C, which is

clearly above T_g (-24°C), an interesting phenomenon was observed, where the spectrum of amorphous xylitol started to undergo a decrease in peak intensity, but without new peaks appearing, as one would normally expect in amorphous-crystalline transition (Fig. 2). Peak intensities decreased for 25 min, when no distinct spectral features could be observed. After this, the characteristic peaks of crystalline xylitol started to gradually appear. A similar phenomenon could be also seen at a temperature of 28.5 – 29.5°C (data not presented). When the same sample was inspected visually, it was observed that after preparation the sample was opalescent. The sample started gradually to become transparent after which the sample gradually turned opalescent again. Also Lakio et al. (2015) have reported material turning transparent. This phenomenon has been associated with high molecular mobility and particle fusion in the rubbery state, i.e. above the glass transition temperature (Slade and Levine, 1991; Hancock and Zografi 1997). In the rubbery state the high molecular mobility means that crystallization is also likely (Slade and Levine, 1991; Hancock and Zografi, 1997).

With the WAXS measurements at 29.0 ± 0.3°C (measurements were not performed at the 20.1 – 21.6°C, due to sampling setup limitations), the first peaks were seen at 5 min and the intensity increased rapidly (Fig. 3). During the experiment, the peak positions did not change, which indicates that the unit cell dimensions of crystalline xylitol remained unchanged and there were no polymorphic transitions between different crystal polymorphs.

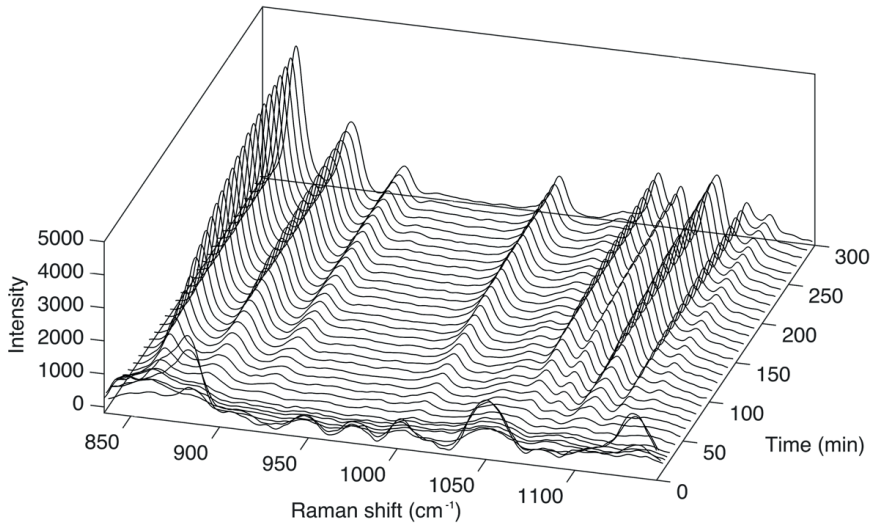

Fig. 2. Raman spectra of crystallizing xylitol at 20.1 – 21.6°C. For 0 – 20 min the spectra shown are every 4 min and for 20 – 300 min every 10 min. The figure is reproduced from paper **I**, with the permission of Elsevier.

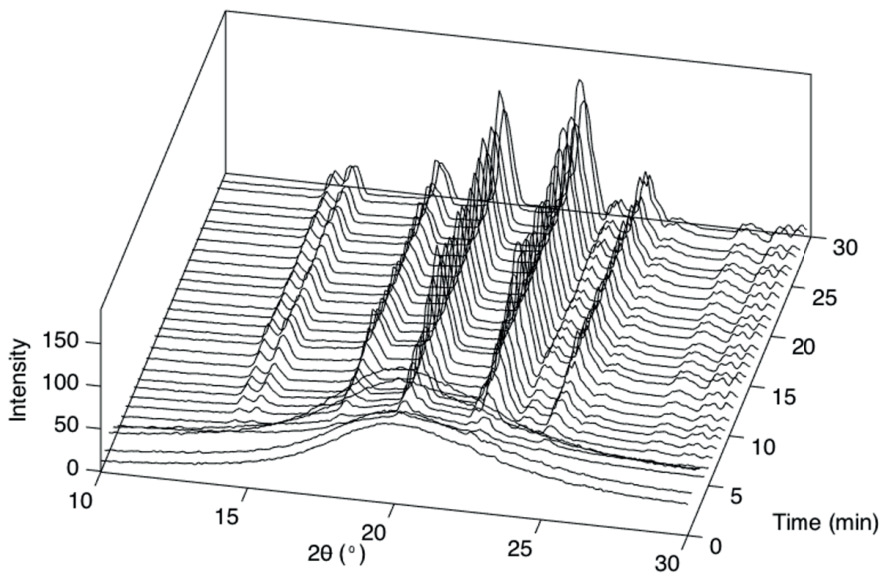

Fig. 3. X-ray diffractograms of crystallizing xylitol at 29.0 ± 0.3. Diffraction patterns shown were taken every 1 min for 30 min. The figure is reproduced from paper **I**, with the permission of Elsevier.

The WAXS measurement, however, suggested the recrystallization rate of amorphous xylitol in the absence of the silica was faster than the recrystallization rate of xylitol in the amorphous xylitol-silica dispersion (Fig. 4), which is the opposite to that observed with the Raman measurements (Fig. 5a).

The differences between the Raman spectroscopy and WAXS results can be explained by two factors, of which the second one is different to that discussed in article **I**.

Firstly, when comparing the measurements of xylitol-silica dispersions, the Raman spectroscopy results suggest crystallization starts earlier than with the WAXS measurements. This can be explained by different sensitivities to length-ranges of order. Shorter-range order can be detected with Raman spectroscopy, since the technique is sensitive to both intra- and intermolecular vibrations. In contrast, WAXS detects longer range order on the order of several unit cells. Consequently, Raman spectroscopy is theoretically more sensitive to the nucleation and very small nanocrystals, which are present at the initial stages of crystallization.

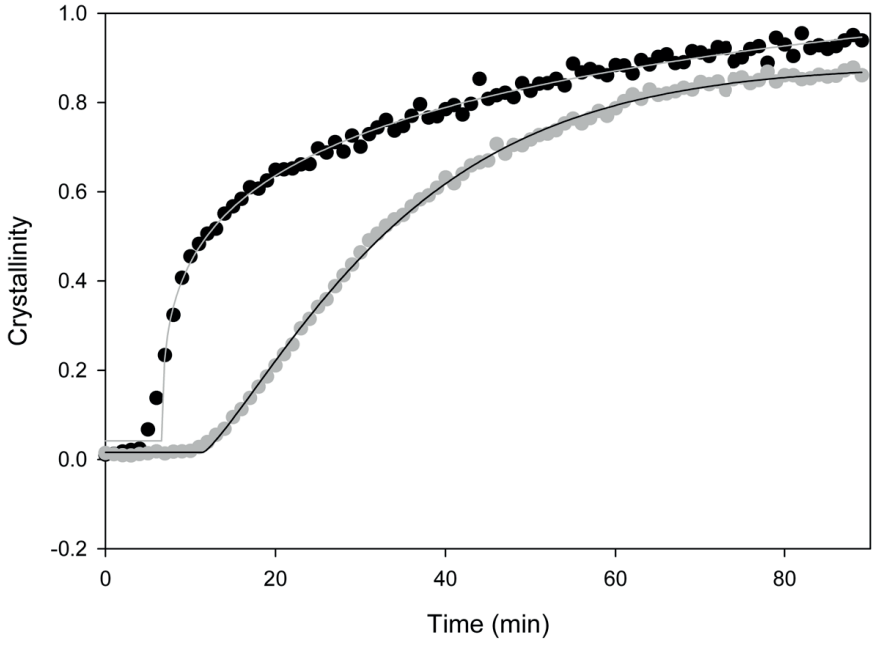

Fig. 4. Crystallization of amorphous xylitol (black) and amorphous xylitol in the amorphous xylitol-silica mixture (grey) measured with WAXS at 29.0 ± 0.3°C. The figure is reproduced from paper **I**, with the permission of Elsevier.

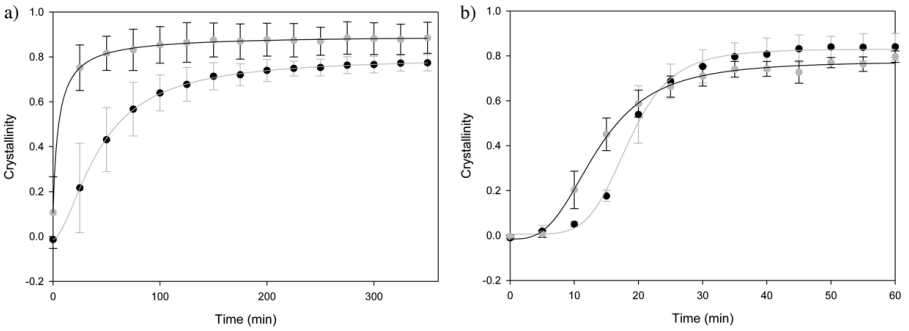

Fig. 5. Averaged crystallization curves of crystallization of amorphous xylitol alone (black) and amorphous xylitol in xylitol-silica mixture (grey) measured using Raman spectroscopy in a) ambient conditions (T = 20.1 – 21.6°C and RH% = 21 – 36) and b) elevated temperature conditions (T = 28.5 – 29.5°C and RH% = 19 – 25). The figure is reproduced from paper **I**, with the permission of Elsevier.

Secondly, when comparing the onset of xylitol crystallization in pure xylitol samples, the crystallization appeared to start earlier with WAXS analysis than with Raman analysis. This was not expected based on earlier studies at

temperatures below T_g (Ueda et al., 2014; Mah et al., 2014), as well as the xylitol-silica mixture results and interpretations (different sensitivities of WAXS and Raman to lengths of order) described above. However, the differences in crystallinity detected by Raman and WAXS in the pure xylitol samples can be explained by the transparency of the samples. With increased transparency, fewer Raman scattered photons are directed back to the sampling probe and hence detector. Furthermore, the opportunity for Raman scattering is decreased due to the lower degree of elastic (back) scattering of the laser photons within the sample. So, even though the crystallization could have already started, nanocrystals smaller than the wavelength of the light would mean that the sample it is not yet opaque and consequently any Raman scattering from the small crystals is not sufficiently directed back to the probe and detector. It is at this stage, that the overall Raman signal is very weak with a lack of visible peaks. Since the effect of opacity (or lack thereof) in the Raman signal strength overrides any detection of xylitol crystallization, the Raman analysis is not reliable during early crystallization. Thus, only the WAXS results are further discussed when comparing the crystallization of xylitol in pure xylitol samples and amorphous xylitol-silica dispersions. The Raman analyses are more robust in the mixtures, since silica is of a sufficiently large particle size (larger than the wavelength of the laser light) that it elastically scatters the laser light and keeps the sample opaque.

Watanabe et al. (2001) have made amorphous indomethacin-silica dispersions using melting and quench cooling. In those dispersions, the silicon dioxide decreased the crystallization rate by forming interactions between the hydroxyl groups of indomethacin and the polar groups of silica. Also, co-grinding clopidogrel and silicon dioxide made clopidogrel more stable by hydrogen bonding between the silanol groups of silicon dioxide and the drug molecule (Mártha et al., 2014). Considering the molecular structure, molecular bonding between polar groups of silica and xylitol could have caused a decreased crystallization rate in the xylitol-silica dispersion in the present study (Watanabe et al., 2001; Takeuchi et al., 2005; Xu et al., 2013; Mártha et al., 2014). If the amount of silica used in dispersion is small, as it was in the xylitol-silica dispersions in this study, drug loading into pores is very limited. However, as mentioned above, interactions between the external silica particle surfaces could also stabilize the amorphous form and thus explain why the end-state crystallinity of xylitol-silica dispersions is lower than in crystallized pure amorphous xylitol.

To conclude, based on WAXS measurements, the overall crystallization rate of xylitol-silica dispersion was decreased over a prolonged period of time compared to that of pure xylitol. Additionally, it could be clearly seen that Raman spectroscopy is not the most suitable method, when measuring samples that exhibit changes in opacity to light in the visible/near-infrared wavelength range (in this case, above the sample T_g).

5.1.2 COMPARISON OF SPECTRAL PRETREATMENTS USED BEFORE MULTIVARIATE ANALYSIS

This section considers which pre-treatments should be used when performing quantitative Raman spectroscopic analysis of xylitol crystallinity in pure xylitol samples, as well as in xylitol-silica dispersions. In this study, 36 pretreatments or pretreatment combinations (including one with no pretreatments) were compared based on the accuracy of the PLS model created after the treatments.

Many publications such as those by Fearn et al. (2003), Igne et al. (2010), Blanco et al. (2000,2007), Gaydou et al. (2011), Faber et al. (1999), Zhou et al. (1998) and Vanarase et al. (2010), have discussed the use of PLS models and pretreatments that are beneficial for the accuracy of the models covering a few pretreatments and some of them even a few combinations of pretreatments. However, these studies have investigated a more limited range of pretreatments and their combinations compared to extensive number of pretreatments and their combinations presented in figure 6.

To know if there needs to be separate models for crystallization of xylitol alone and in dispersion with silica, the effect of silica on the Raman spectra was investigated. Silica did not have significant peaks, but a rather a broad area of increased intensity, which is likely caused by fluorescence. Additionally, in the spectral region used in the PLS model barely affects the shape of the spectra (Fig. 7). Consequently, the effect of silica on the spectra could be excluded using baseline correction. Therefore, using a single model for both types of Raman spectroscopic samples was justified.

When the Raman spectra of amorphous and crystalline xylitol were compared, overlapping peaks were evident (Fig. 7). Additionally, there were baseline and intensity variations, which may have been caused by differences in sample packing, density and particle size (Pellow-Jarman et al., 1996; Savolainen, 2008). Consequently, peak intensity or area comparison was not possibility. It has been reported that multivariate PLS models can have significantly smaller root mean square errors than models based on single peak heights or areas (Johansson et al., 2005). In addition to selecting multivariate analysis to be used in crystallinity determination, extensive work was done to discover which pretreatment methods should be done to the spectral data before the PLS modelling (Fig. 6). In this thesis, this part of the study is presented more widely than in article **I**, where most of the results in this section can be seen.

To select the best pretreatment or pretreatments to be used, spectra were subjected to various pretreatments, the PLS models were constructed and their goodness (R^2) and predictability (Q^2) were compared. The results can be seen in table 1.

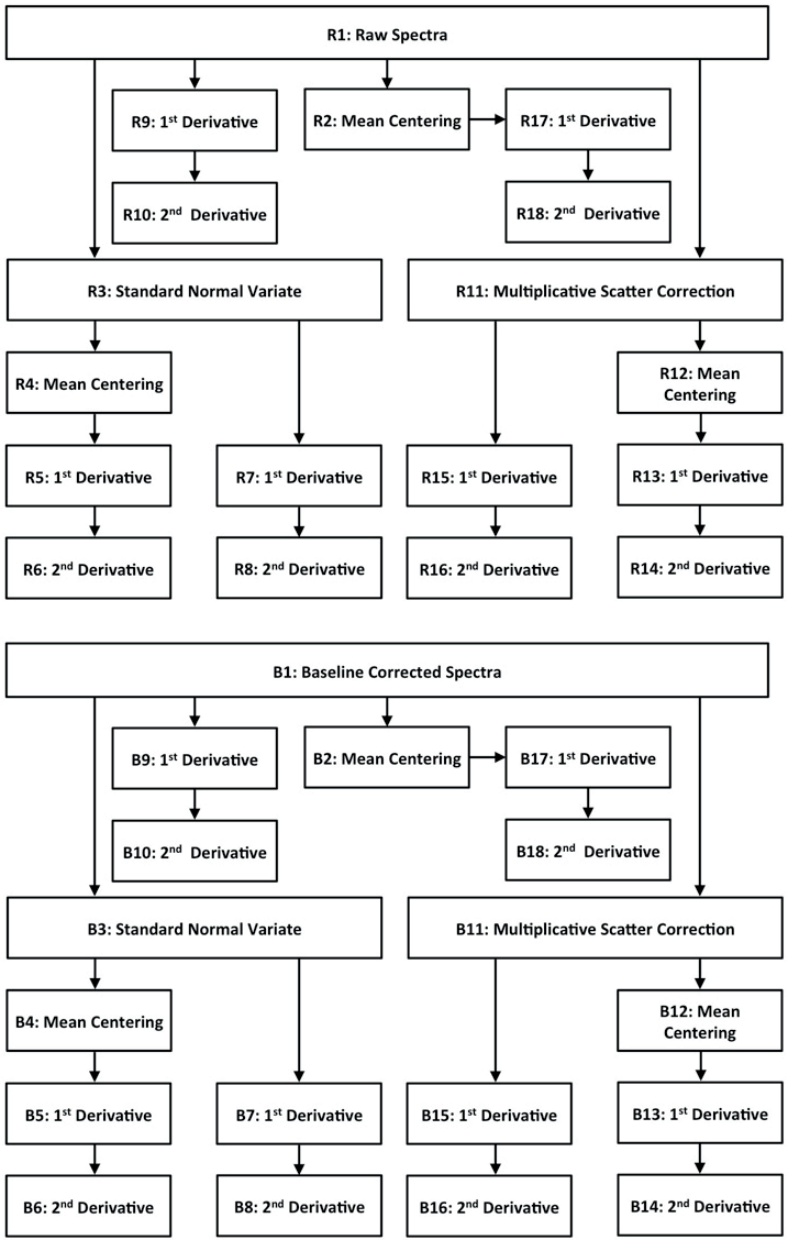

Fig. 6. Pretreatment methods for the spectral data. Reproduced from conference paper (Palomäki et al., 2016).

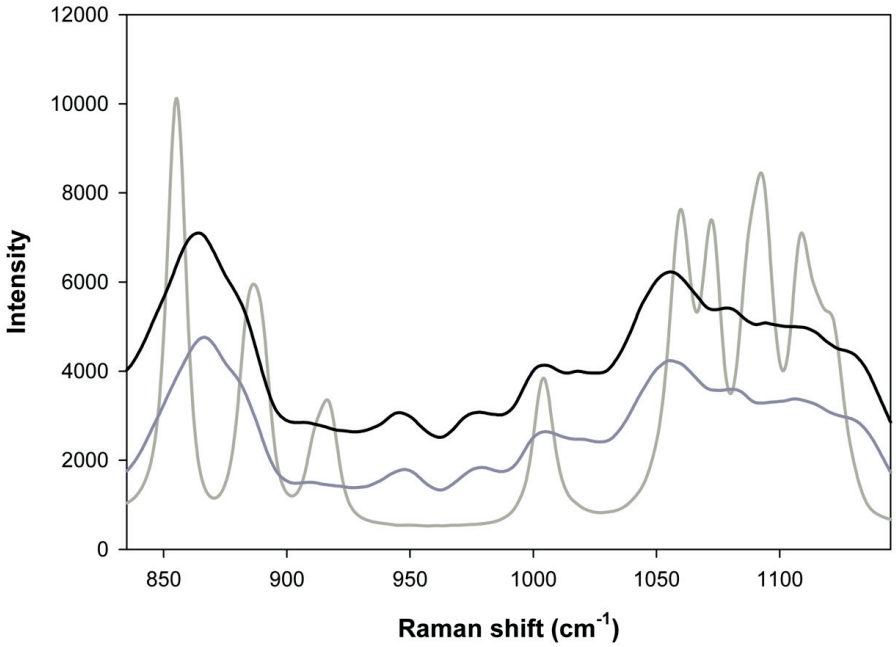

Fig. 7. Spectra of crystalline xylitol (light grey), amorphous xylitol (dark grey) and amorphous xylitol with 10% silica (black). The spectral region is the same as that used in the PLS model.

Table 1. Effect of pretreatments on the goodness of model (R^2) and its predictability (Q^2). Reproduced from conference paper (Palomäki et al. 2016).

Pre	R^2	Q^2	Pre	R^2	Q^2
R1	0.881	0.876	B1	0.932	0.927
R2	0.281	0.270	B2	0.284	0.275
R3	0.963	0.963	B3	0.940	0.938
R4	0.298	0.285	B4	0.292	0.282
R5	0.294	0.282	B5	0.286	0.272
R6	0.909	0.904	B6	0.832	0.821
R7	0.909	0.906	B7	0.866	0.861
R8	0.971	0.969	B8	0.876	0.871
R9	0.934	0.928	B9	0.857	0.855
R10	0.932	0.927	B10	0.932	0.927
R11	0.880	0.862	B11	0.800	0.793
R12	0.898	0.895	B12	0.906	0.885
R13	0.293	0.278	B13	0.270	0.234
R14	0.293	0.279	B14	0.259	0.222
R15	0.967	0.966	B15	0.923	0.921
R16	0.972	0.970	B16	0.931	0.927
R17	0.279	0.261	B17	0.278	0.251
R18	0.277	0.230	B18	0.277	0.229

Even without pretreatments (Table 1: R1), the PLS model had fairly good R^2 and Q^2 values. Because the baselines were not straight and since there can be fluctuations in overall spectral intensity due to measurement artefacts unrelated to the sample composition (e.g. laser intensity, sample positioning), some preprocessing is preferable. In this study, baseline correction with rubberband correction (Table A: B1) and Savitzky-Golay 2nd derivatives (Table A: R10) led equally good PLS models. However, if some other additional preprocessing was done, Savitzky-Golay 2nd derivatives produced better results. The best model was achieved using MSC-correction and Savitzky-Golay 2nd derivatives (Table A: R16) with R^2=0.972 and Q^2=0.970. An almost equally good model was obtained using SNV-correction, Savitzky-Golay 2nd derivatives (Table A: R8) with R^2=0.972 and Q^2=0.970. Other good models (R^2>0.95 and Q^2>0.95) were obtained using the following pretreatments: MSC and Savitzky-Golay 1st derivatives (Table A: R15) having R^2=0.967 and Q^2=0.966 and SNV (Table A: R3) having R^2=0.963 and Q^2=0.963.

Since the data had intensity fluctuation and baseline variation, it was not surprising that commonly used 2nd derivatives, MSC and SNV were found to be good pretreatment methods (Johansson et al., 2005; Strachan et al., 2007; Rinnan et al., 2009). The 2nd derivative treatments remove baseline shifts and linear trends (Rinnan et al., 2009). The SNV and MSC remove additive and multiplicative errors and often produce very similar outcomes. It has to be taken in account that MSC requires external reference spectra, which is often the average of a calibration set. Even though certain spectral pretreatments seemed to be superior to others, it cannot be stated that some of them should be exclusively used. In Raman spectroscopy, spectral data can have variations caused by fluorescence, particle size, sample packing, instrument reproducibility and intensity variation (Heinz et al., 2007; Pellow-Jarman et al., 1996), which might affect which pretreatments are preferred for a specific measurement set. However, using SNV or MSC with Savitzky-Golay 2nd derivatives as pretreatments will mostly lead to good PLS models, provided the data itself is of sufficient quality and contains the required information.

It is important to note the optimal spectral pretreatments were selected based on the calibration sets. These samples were prepared by melting and quench cooling xylitol and adding a specific amount of crystalline xylitol prior to cryo-grinding. The material was ground and liquid nitrogen was evaporated. The same samples were also used as the test set (cross-validation). An equally important and often challenging additional consideration is any differences between the calibration set, and the samples that the model is subsequently applied to, in this case, the crystallization samples presented in the previous section. While the calibration sets can be considered valid for the opaque samples, the changes associated with changing opacity have not been explicitly incorporated into the quantitative model development. In this case, the changing opacity during crystallization represents a further challenge for the development and application of quantitative models, which should be more deeply explored in future work.

5.2 EFFECT OF ATMOSPHERE ON THE ONSET OF CRYSTALLIZATION OF SLOWLY COOLED PARACETAMOL MELT (II)

In this section, results regarding the second research objective, involving the effect of atmospheric gases on the onset of crystallization of amorphous API, are presented. Contrary to the pure xylitol samples in study **I**, Raman spectroscopy is a good method to be used in study (**II**), since the samples did not turn transparent.

The amorphous samples in article **II** were first melted and then slowly cooled and not ground. Crystallization was monitored using Raman spectroscopy and the end state polymorphic form was confirmed using X-ray diffraction. According to Raman spectroscopy and WAXS results, these amorphous samples subsequently crystallized to form II at all temperatures (17.2 ± 0.3°C, 21.7 ± 0.2°C, 23.9 ± 0.4°C and 27.5 ± 0.2°C) and in all atmospheres (N_2, CO_2, dry air and moist air). When amorphous samples were prepared similarly and investigated with DSC (Fig. 8), the onset of the T_g was 22.3 ± 0.1°C, samples started to crystallize at 65.8 ± 0.3°C and the T_m was 157.8 ± 0.2°C, which indicates, that it had crystallized to form II (Di Martino et al., 2000).

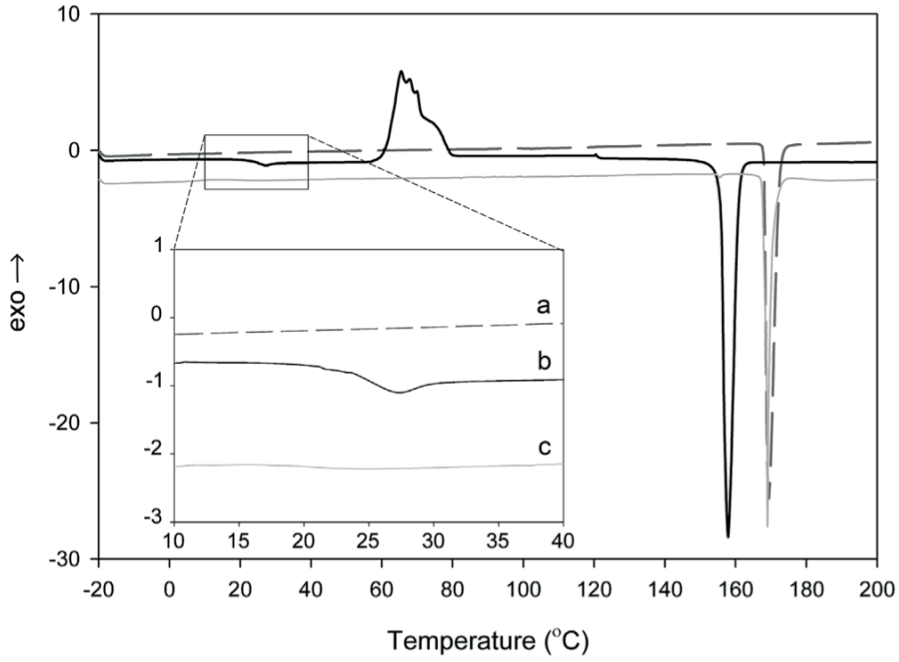

Fig. 8. Typical DSC thermograms of a) paracetamol form I reference sample (dark grey, dashed), b) amorphous paracetamol (black) and c) paracetamol sample that had crystallized during storage (light grey). The figure is reproduced from paper **II**, with the permission of Elsevier.

However, DSC measurements of paracetamol samples that crystallized during stability studies (regardless of atmosphere), contradictory to Raman spectroscopy and WAXS results, showed a melting peak at 169.0 ± 0.1°C (Fig. 8), which corresponds to the melting point of paracetamol form I (168 – 172°C) (Di Martino et al., 1996, 1997, 2000; Nichols and Frampton, 1998). Qi et al. (2008) reported a similar phenomenon. In their study, the quench cooled sample of paracetamol form II, paracetamol converted into form I during DSC measurement in nonisothermal conditions, which was detected with Raman spectrometry, but could not be seen in the DSC diffractogram. No exothermic recrystallization prior to melting could be seen in the thermogram, which is in line with Kauffman et al. (2008) and Di Martino et al. (1996). Kauffman et al. (2008) used Raman spectroscopy and DSC simultaneously to measure aging of paracetamol form II. In their study, paracetamol converted from form II to form I without showing evidence of recrystallization in the thermogram. Di Martino et al. (1996) had similar results, when investigating samples, which were confirmed to be form II using X-ray, which converted to form I during DSC measurement without showing evidence of such a transition in the thermogram. Consequently, DSC is not an optimal method for investigating polymorphism of paracetamol.

The effect of headspace gases on onset of crystallization of amorphous paracetamol depended on storage temperature (Fig. 9). At 17.2 ± 0.3°C, the onset of crystallization of amorphous paracetamol was delayed in dry air compared to dry nitrogen or dry carbon dioxide. The higher the temperature was, the less obvious the difference between the onset of crystallization was. Zografi and Newman (2017) detected that below T_g non-relaxed samples absorbed more water than relaxed samples, but they did not detect similar behavior above T_g. Any other gas with a tendency to interact with the amorphous surface could be expected to interact similarly to water.

Temperature has an important role in the adsorption of gases onto surfaces, dissolution at the surface and diffusion into the matrix. At lower temperatures, more adsorption takes place. Additionally, the solubility of gases in solids is higher at lower temperatures (Chaix et al., 2014). According to the Stokes-Einstein equation, the diffusion coefficient is directly proportional to temperature and inversely proportional to size of the gas molecules and viscosity of the amorphous matrix. A higher temperature would increase molecular motion and reduce viscosity. This would lead to increased molecular mobility and diffusion of the gas from the surface to the bulk. This may reduce build-up of the gases on the surface of the glassy matrix. Since the recrystallization is more surface-driven below T_g and a lower viscosity of the surface compared to bulk is needed for surface-biased crystallization (Yu et al. 2016), temperature may play a key role in solid-gas interactions of amorphous systems. Indications of this were also seen in the present study (Fig. 9), where the changes in dry gaseous environment were found to have a more pronounced effect on crystallization at lower temperatures.

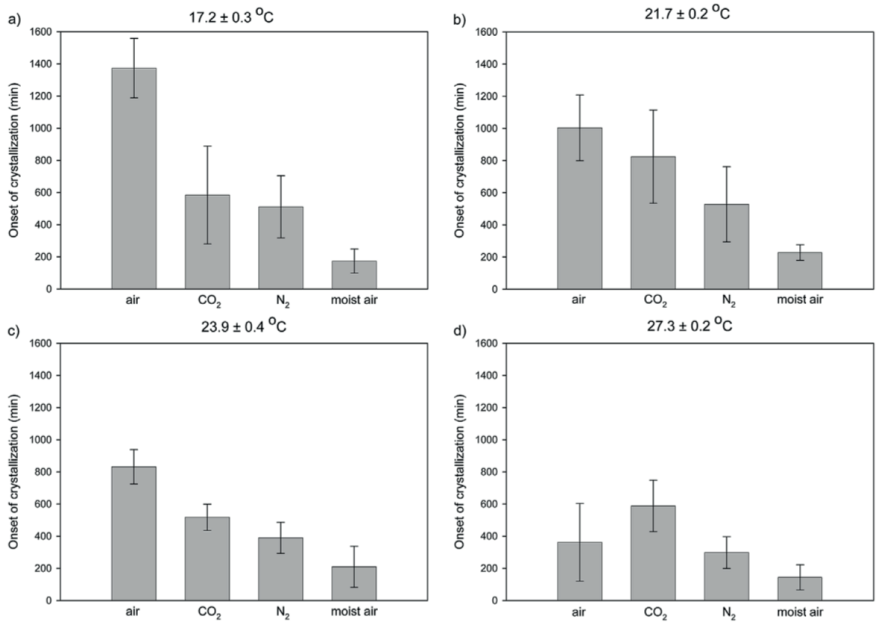

Fig. 9. Average onset of crystallinity for paracetamol in different temperatures and atmospheres. The figure is reproduced from paper **II**, with the permission of Elsevier.

At the T_g and above, amorphous material becomes a super-cooled liquid, in which surface crystallization is less dominant over bulk crystallization. This is consistent with no difference being seen in crystallization onset times between different atmospheres above T_g. At the highest temperature at 27.5 ± 0.2°C in all atmospheres, except in moist air, lag times were not constant and the crystallization rates had multiple phases where the crystallization rates fluctuated. In all other environments, crystallization followed a typical sigmoidal curve with one period of increasing crystallization rate, steady state of crystallization rate and one period of decreasing crystallization rate. Additionally, there was notable variation between samples, which is also consistent with observations by Yu et al. (2016), in which crystallization kinetics of amorphous materials were found to vary between samples at temperatures above T_g to that below T_g (Fig. 9).

In this study, paracetamol crystallized faster in humid air compared to dry air. Amorphous materials are hygroscopic and are plasticized by humidity resulting in a lower T_g and higher molecular mobility (Hancock and Zografi 1994). As a result, when relative humidity rises, the crystallization rate also increases (Lehmkemper et al., 2017; Hoppu et al., 2007). Still, differences in moisture content cannot explain the differences in crystallization onset between dry air and other dry atmospheres, when the amount of water in gas and collisions to sample surfaces are considered (Table 2). Additionally, no effect of humidity on crystallization rate of dry samples was seen in the Avrami constant *n*, when crystallization curves were fitted with Avrami equation.

Consequently, water alone does not explain the difference in crystallization onset times of amorphous paracetamol in dry air and nitrogen.

Table 2. Amount of water in various gas mixtures and collision frequency of water molecules. Calculations assume a temperature of 20°C and normal atmospheric pressure. The table is reproduced and edited from paper **II**, with the permission of Elsevier.

Atmosphere	RH%	H_2O (g/m^3)	H_2O (m/m-%) in the atmosphere	Theoretical amount of collisions between gaseous H_2O molecules and the sample surface ($n/Å^2/s$)[a]
Air	4.4-4.7	0.76-0.81	0.06	4200-4400
CO_2	1.2-1.5	0.21-0.26	0.02	1100-1400
N_2	≤0.1	≤0.2	0.0	≤ 100
Humid air	21.2-22.2	3.67-3.85	0.29-0.30	20000-21000

[a] Collision frequency (Atkins 1998, Jensen 2007)

Amorphous materials and gases may interact with each other via intermolecular interactions (Byrn et al., 2001; Buckton and Gill, 2007; Manca et al., 2003), so the assumption of pure Fickian penetrant diffusion of gases is invalid in the present study. Attractive interactions between gas and molecules in amorphous substance would lead to accumulation of gas molecules in the surface layers of the sample.

It has been shown, that amorphous and liquid paracetamol have hydrogen bonds between the phenolic hydroxyl and amine groups and between the phenylic hydroxyl and carbonyl oxygen (Gunawan et al., 2006). Hydrogen bonding even has an effect on the structural relaxation of the glass (Gunawan et al., 2006). Additionally, if stronger hydrogen donors or acceptors interfere with hydrogen bonds between paracetamol molecules, the amount of crystal nuclei formation is reduced (Trasi and Taylor 2012). Since at the surface there are functional groups that are in contact with the gas phase and are not interacting with functional groups of the other molecules, one could assume that the molecules could interact with headspace gas molecules, and these interactions could potentially have an effect on crystallization. The results of this study support this hypothesis.

On the sample surface, amorphous paracetamol molecules are more randomly arranged than with a crystalline substance (though there may be some short-range order) and various functional groups are presented to the gaseous phase. It can be assumed that amine, phenolic hydroxyl and carbonyl oxygen, that have tendencies to form molecular bonds, would interact especially with O_2 and also with N_2. N_2 is less reactive due to the triple bonding compared to O_2 with double bonding. Interacting gas molecules adsorbed on to the surface layer may slow down nuclei formation and consequently, cause a delay in the onset of crystallization. This is supported by Manca et al. (2003),

who found that N_2 and CO_2 were adsorbed site-specifically onto the surface of amorphous ice. Since these kinds of interactions cannot be detected using Raman spectroscopy, it was not possible to get direct evidence of similar site-specific bonding in the present study, but the phenomenon cannot be excluded.

There was some variation between onsets of crystallization between similar samples in the present study. They may have had some spatial and dynamic heterogeneity (Ediger, 2000, Sillescu 1999), which would lead to differences in the time required for stable nuclei to form and would, consequently, cause variation in lag-time before the onset of crystallization. In the present study, such heterogeneous nucleation occurred at the gas-amorphous-glass slide interface as described in section 5.1.3.

To conclude, physisorption is known to occur more at low temperatures through intermolecular interactions at active sites. As the temperature is decreased, adsorption and dissolution of gases into the amorphous material increase while the decrease in temperature makes the material become more viscous in the bulk compared to the surface. When, at the same time, also the tendency of surface crystallization increases, it can be summarized that the onset of crystallization of amorphous paracetamol is expected to be affected by atmospheric gases below T_g, as shown in the present study. Above T_g a similar effect was not seen.

5.3 ALTERING THE RECRYSTALLIZATION OF AMORPHOUS MATERIALS IN THE PRESENCE OF DIFFERENT EXCIPIENTS (I, III)

In this section, the third research objective, which considers the effect of excipients on crystallization of two-phase amorphous solid dispersions, is addressed. The section explores potential stabilization with two-phase systems in more detail from a mechanistic perspective.

In study **I**, silica was added to influence the crystallization of amorphous xylitol. In this case, the silica is not expected to mix with the xylitol on a molecular/atomic level, and thus the two phases (silica and xylitol) can be considered chemically pure. Furthermore, the silica is effectively physically stable in the amorphous form and not liable to crystallization itself. Crystallization of xylitol could be affected by mechanical inhibition of crystal growth and molecular interactions at the xylitol-silica interfaces. In study **III**, both API and excipient are small molecules, and both materials are liable to crystallization. In this case, in addition to mechanical inhibition of crystallization and molecular interactions at the phase interfaces, there can be some API molecules in the excipient-rich phase and vice versa in a two-phase system (resulting in API-rich areas and excipient-rich areas). Consequently, there is some level of molecular level mixing, which can further inhibit

crystallization. In addition, crystallization of either component could subsequently influence crystallization of the other component.

As mentioned above, the first two-phase solid dispersion system investigated included xylitol and non-ordered mesoporous silica, in which only the xylitol was expected to crystallize (**I**). In the study, pure xylitol crystallized faster than the xylitol-silica solid dispersion (based on WAXS analysis, since Raman was not suitable for analysis of the pure xylitol). These results have already been presented in section 5.1.1. Qualitative differences in xylitol samples before and after crystallization were explored in this section with polarizing light microscopy and DSC.

In the polarizing light microscopy images (Fig. 10), the crystallite size appeared much smaller in the solid dispersion than in xylitol alone. It appears that the presence of the silica prevented larger crystals from growing, which is consistent with the lower crystallization rate of xylitol in the xylitol-silica dispersion compared to xylitol alone.

DSC can offer insights into whether the molecular mobility of the xylitol is affected by the presence of the mesoporous silica. In the DSC measurements in article **I**, amorphous xylitol and amorphous xylitol-silica dispersions showed a T_g for amorphous xylitol (Fig. 11). The onset of the T_g for xylitol was at -23.3°C, which is well in line with earlier findings of Talja and Roos (2001), in which the stated T_g of waterless xylitol was -24°C. The slight difference is likely due to different heating rates. The T_g was followed by a wide exothermic peak corresponding to recrystallization of amorphous xylitol and sharp endothermic melting peak (92 – 96°C).

The onset of T_g for xylitol in the xylitol-silica dispersion was -32°C, which is significantly lower than the T_g of xylitol alone. Additionally, the glass transition occurred over a larger temperature range than with pure xylitol. Talja and Roos (2001) have earlier reported that water content significantly affects the T_g of xylitol (as would be expected due to water being a plasticizer), and xylitol samples containing 10% of moisture had T_g of -53°C. Hygroscopicity of silica explains lowering of the T_g compared to pure xylitol, which would promote crystallization. Amorphous sucrose has previously been stabilized using micro-sized filler particles (Hellrup and Mahlin, 2011). However, the stabilizing effect of the microparticles was lost, when the relative humidity exceeded a critical threshold. As mentioned above, any moisture in the sample would act as a plasticizer, and thus increase molecular mobility and counteract the stabilizing effect of silica (Andronis et al., 1997; Hellrup and Mahlin, 2011). However, in the present study with xylitol, this effect appears to be more than compensated for by the potential interface interactions between silica and xylitol and/or steric hindrance, since silica slows down crystallization according to WAXS.

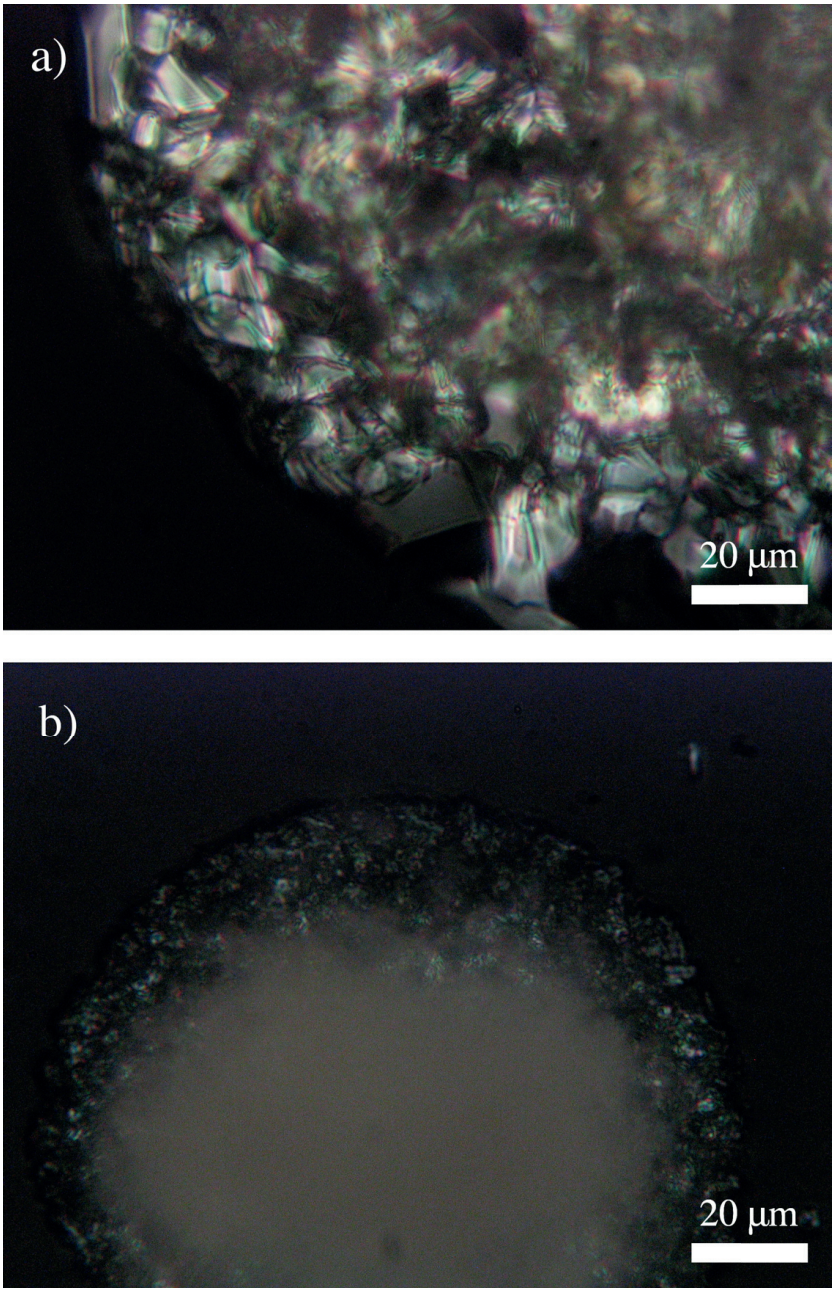

Fig. 10. Polarizing light microscope images of ground a) xylitol and b) xylitol-silica dispersion after crystallization of xylitol. The figure is reproduced and edited from paper **I**, with the permission of Elsevier.

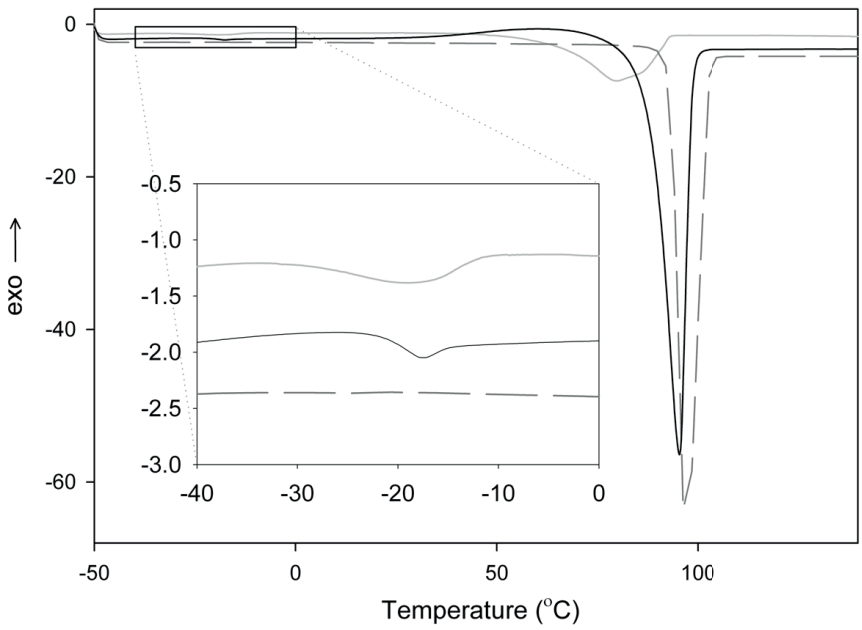

Fig. 11. Typical DSC thermograms of mixture of amorphous xylitol and silica (light grey), amorphous xylitol (black) and crystalline xylitol (dark grey, dashed). The figure is reproduced from paper **I**, with the permission of Elsevier.

In article **III**, paracetamol was mixed with another small molecule, either trehalose or melibiose, resulting in two-phase amorphous systems, as revealed with XRPD. Two small molecule components would theoretically allow some degree of molecular-level mixing upon melting. Despite this, any mixing was limited, as evidence of the two-phase nature was provided by both FTIR and DSC.

When FTIR results of the amorphous solid dispersions of paracetamol-melibiose or paracetamol-trehalose were compared to predicted spectra calculated from the weighted average of the amorphous paracetamol spectrum and either amorphous melibiose or trehalose, the spectra were almost identical. This indicates that the solid dispersions lacked significant drug-excipient intermolecular interactions, such as H-bonding, and may have existed as two-phase systems.

The two-phase nature was confirmed with DSC. With both the amorphous paracetamol-trehalose and paracetamol-melibiose dispersions, there were two T_gs instead of one (Table 3). The first T_g, at 17.9 ± 0.5°C, corresponded to that of the paracetamol-rich phase and the second T_g to those of the excipient-rich phases. This paracetamol-rich phase T_g is lower than that of the pure drug, in contrast to what would be expected upon any mixing with either excipient according to Gordon-Taylor behavior. The T_g is lowered likely because of the hygroscopicity of melibiose and trehalose, and thus water absorption into the

system. Even though samples were amorphized in a nitrogen atmosphere, the humidity getting into contact with sample upon rapid cooling of the melt with liquid nitrogen and also DSC sample preparation could not be totally prevented.

Table 3. Endo- and exothermic reactions in DSC measurements (n=3, $\bar{x} \pm$ sd).

	T_gs (midpoint) (°C)	Onset of crystallization (°C)	Melting endotherm(s) (°C)
Amorphous paracetamol	24.7±0.2	57.5±0.7	171.7±0.3
Amorphous melibiose	88.5±0.2	NA	NA
Amorphous trehalose	117.5±1.0	NA	NA
Crystalline paracetamol	NA	NA	171.3
Crystalline melibiose	NA	NA	189.1
Crystalline trehalose	NA	NA	213.4
Solid dispersion: paracetamol 25%, melibiose 75%	17.9±0.5, 79.8±0.9	117.2±1.2	164.2±0.7
Solid dispersion: paracetamol 25%, trehalose 75%	18.0±0.4, 97.1±0.4	135.7±2.7	166.2±0.1, 204.0±0.4

In the paracetamol-trehalose and paracetamol-melibiose dispersions both T_gs corresponding to the disaccharides, melibiose and trehalose, were also lowered compared to the T_gs of the pure excipients (without paracetamol) right after preparation. This is likely to be caused by the sugars' tendency to absorb water during storage, especially in the amorphous phase (Hancock and Dalton 1999), which would lower the T_g remarkably (Liu et al., 2006; Schebor et al., 2010). Additionally, since the T_g of paracetamol (in this study 17.9 ± 0.5 °C) is lower than those of trehalose or melibiose, and there may have been some limited mixing of the components, which would further serve to lower the T_gs (according to Gordon-Taylor behavior).

Even though there were two T_gs in each dispersion and thus two phases were present, the onsets of crystallization in the DSC thermograms for paracetamol in the dispersions were remarkably different compared to that of paracetamol alone (without any excipient). Amorphous paracetamol alone had an onset of recrystallization at 57.5 ± 0.7°C, while in the paracetamol-melibiose mixtures it crystallized at 117.2 ± 1.2°C and in the paracetamol-trehalose mixtures it crystallized at 135.7 ± 2.7°C. These findings are consistent with the storage study results. It is interesting to note, that there was only a single crystallization exotherm in the thermograms, despite two phases existing. However, crystallization exotherms were not present in the thermograms for trehalose or melibiose in pure form.

These two-phase systems were subjected to accelerated stability testing conditions, with a relative humidity of 75% and temperature of 38 ± 0.5°C. The sample crystallization was detected using WAXS and it was seen that samples

crystallized to paracetamol form I. Crystallinity was determined by peak heights at 9.8° 2θ for crystalline melibiose, 14.6° for trehalose dihydrate and 18.2° for paracetamol form I. Ground pure amorphous paracetamol crystallized immediately, while the two disaccharides crystallised more slowly, with onsets of crystallization of 3 hours for trehalose and more than 6 hours for melibiose (Figure 12).

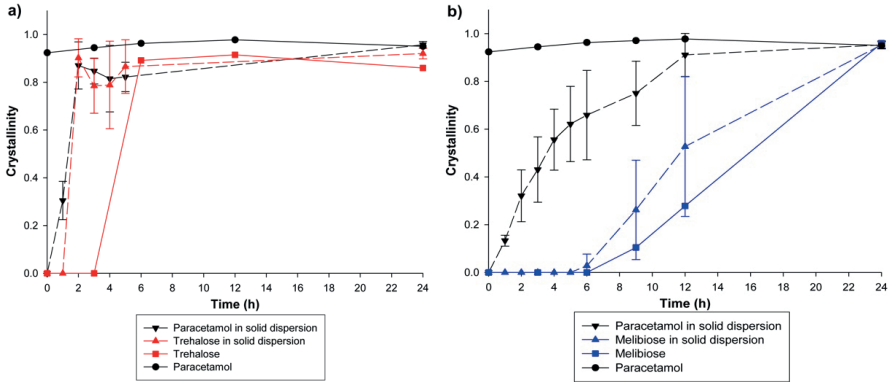

Figure 12. Crystallization of a) amorphous paracetamol alone (black circles), amorphous trehalose alone (red squares), amorphous paracetamol in paracetamol-trehalose solid dispersion (black, triangles) and amorphous trehalose in paracetamol-trehalose solid dispersion (red, triangles) and b) amorphous paracetamol alone (black circles), amorphous melibiose alone (blue squares), amorphous paracetamol in paracetamol-melibiose solid dispersion (black, triangles) and amorphous melibiose in paracetamol-melibiose solid dispersion (blue, triangles). Samples crystallizing were stored at a relative humidity of 75 ± 1% and temperature of 38 ± 0.5°C.

While neither trehalose nor melibiose postponed the onset of crystallization of paracetamol, they did slow its rate of crystallization — substantially in the case of melibiose. In turn, there was some indication that the crystallization of paracetamol itself may have catalyzed the crystallization (nucleation and/or crystal growth) of the disaccharides, though this effect, if present, was much smaller than the stabilizing effect of the two-phase solid dispersions on the less stable paracetamol. These results suggest that, solid dispersions involving two small molecule compounds, even in the case of two-phase systems, can stabilize the less stable amorphous component.

These observations occurred with the samples exposed to accelerated stability testing conditions (38 ± 0.5°C, 75 ± 1% RH), where the amorphous samples were most likely in the rubbery state. In contrast, at a relative humidity of 3 ± 1% and temperature of 38 ± 0.5°C, in which the samples are expected to be present mainly in the glassy state, no sign of crystallization could be seen in amorphous samples of paracetamol-trehalose and paracetamol-melibiose in any of the samples in 356 days (data not shown), whereas (based on article **II**) pure paracetamol alone can stay amorphous in

dry conditions at the temperature of 16.9 – 27.7°C only for some hours (Fig. 9).

Semjonov et al. (2017) have earlier stated that two-phase system can slow down crystallization. They state that in addition to the level of miscibility (which affects the relative concentrations of the other component in the drug- and excipient-rich phases), steric hindrance and reduction of molecular mobility at interfaces may have a significant role in the stabilization of amorphous material in two-phase systems. The findings in this thesis are consistent with this reasoning, and since trehalose and melibiose had higher T_gs (97.1 ± 0.4°C and 79.8 ± 0.9°C) than paracetamol (17.9 ± 0.5°C) in solid dispersions, molecular mobility reduction at the interfaces is expected to play key role in the stabilization of amorphous paracetamol in solid dispersions with trehalose and melibiose. To conclude, two-phase solid dispersions can slow down crystallization rate and/or postpone crystallization remarkably. Usage of the two-phase systems for stabilizing amorphous systems is expected to become more common in the future. Even though they might be less effective as stabilizers of the amorphous form, they form weaker intermolecular bonds and consequently, may not inhibit drug dissolution as has been observed in some one-phase systems (Semjonov et al., 2018; Surwase et al., 2015).

6 CONCLUSIONS

In the present thesis, new information about the effect of excipient and gas interactions on the onset of crystallization and crystallization processes of amorphous materials was obtained. Such insights are crucial, due to the increasing importance of amorphous materials in pharmaceutical field.

In article **I**, it was found that introducing 10% (m/m) of non-ordered mesoporous silica to amorphous xylitol decreased the overall crystallization rate of amorphous xylitol. It was found that Raman spectroscopy is not a suitable method for crystallinity detection if the transparency of the sample changes, as is prone to happen at temperatures above T_g. The article also demonstrated more in depth than earlier have been reported, the importance of usage of carefully selected spectral pre-treatments prior to multivariate analyses.

In article **II**, the onset of crystallization in different atmospheres was investigated. It was found that at temperatures below T_g, storing amorphous paracetamol samples in dry air delayed the onset of crystallization when compared to samples stored in pure nitrogen. The results imply that oxygen, the gas with reactive nature, was adsorbed onto the surface of the amorphous paracetamol and led to disturbance of the intermolecular interactions between paracetamol molecules. Headspace gases can have a more significant effect on the stability of amorphous pharmaceuticals than previously reported.

In article **III**, two small molecule excipients, trehalose and melibiose, slowed down the crystallization of amorphous paracetamol significantly, when mixed with the drug in a two-phase solid dispersion and stored in elevated temperature and humidity conditions. DSC and FTIR provided evidence that the components exhibited very limited mixing on a molecular level, but despite this, crystallization of the less stable amorphous component was inhibited. Additionally, in some cases two-phase systems could be more useful. Two-phase systems have weaker bonds compared to one-phase systems and consequently, might not inhibit dissolution to a similar degree as stronger intermolecular interactions can in some cases.

Overall, these studies demonstrate that crystallization of material can be interrupted by contact with other molecules, with or without mixing on the molecular level. Thus, while strong bonds between different molecules have long been established as a stabilizing mechanism, these studies show that interactions at interfaces in two-phase systems can also substantially influence crystallization, even without any degree of molecular-level mixing. Furthermore, as the effect of gas on crystallization of amorphous material suggested, also non-specific interactions can affect crystallization.

Crystallization is a process that has been extensively studied, but there are still areas that remain challenging with respect to understanding how different formulation and environmental factors affect crystallization. While this thesis

has provided further insight into these factors, more research is needed to ensure that amorphous materials can be used effectively and safely more often in drug formulations in the future.

REFERENCES

Aaltonen J., Gordon K. C., Strachan C. J., Rades T., 2008. *Perspectives in the use of spectroscopy to characterise pharmaceutical solids*. Int. J. Pharm. 364, 159–169.

Abdul-Fattah M., Lechuga-Ballesteros D., Kalonia D. S., Pikal M. J., 2008. *The impact of drying method and formulation on the physical properties and stability of methionyl human growth hormone in the amorphous solid state*. J. Pharm. Sci. 97, 163–184.

Akao K.-I., Okubo Y., Asakawa N., Inoue Y., Sakurai M., 2001. *Infrared spectroscopic study on the properties of the anhydrous form II of trehalose*. Implications for the functional mechanism of trehalose as a biostabilizer. Carbohyd. Res. 334, 233–241.

Almarsson Ö., Gardner C.R., 2003. *Novel approaches to issues of developability*. Curr. drug deliv. 2, 21–26.

Almarsson Ö., Zaworotko M.J., 2004. *Crystal engineering of the composition of pharmaceutical phases. Do co-crystals represent a new path to improved medicines?* Chem. Commun. 17, 1889–1896.

Alonzo D.E., Zhang G.G.Z., Zhou D., Gao Y., Taylor L.S., 2010. *Understanding the Behavior of Amorphous Pharmaceutical Systems during Dissolution*. Pharm. Res., 27 (4), 608–618.

Amado A.M., Azevedo C., Ribeiro-Claro P.J.A., 2017. *Conformational and vibrational reassessment of solid paracetamol.* Spectrochim. Acta A 183, 431–438.

Andronis V., Yoshioka M., Zografi G., 1997. *Effects of sorbed water on the crystallization of indomethacin from the amorphous state*. J. Pharmaceut. Sci. 86 (3), 346–351.

Artiaga R., Naya S., Garcìa A., Barbadillo F., Garcìa L., 2005. *Subtracting the water effect from DSC curves by using simultaneous TGA data*. Thermochim. Acta 428, 137–139.

Asmus L.R., Kaufmann B., Melander L., Weiss T., Schwach G., Gurny R., Möller M., 2012. *Single processing step toward injectable sustained-release formulations of Triptorelin based on a novel degradable semi-solid polymer*. Eur. J. Pharm. Biopharm. 81, 591–599.

Atkins P.W., 1998. *Physical Pharmacy*, sixth ed., Oxford University Press, Oxford, 835.

Baghel S., Cathcart H., O'Reilly N.J., 2016. *Polymeric Amorphous Solid Dispersions: A Review of Amorphization, Crystallization, Stabilization, Solid-State Characterization, and Aqueous Solubilization of Biopharmaceutical Classification System Class II Drugs*. J. Pharm. Sci. 105, 2527–2544.

Berthomieu C., Hienerwadel R., 2009. *Fourier transform infrared (FTIR) spectroscopy*. Photosynth. Res. 101, 157–170.

Beyerinck R.A., Ray R.J., Dobry D.E., Settell D.M., 2003a. *Method form making homogeneous spray-dried solid amorphous drug dispersions using pressure nozzles*. Patent WO03/063821A2.

Beyerinck R.A., Ray R.J., Dobry D.E., Settell D.M., Spence K.R., 2003b. Deibele H.L.M., *Method for making homogeneous spray-dried solid amorphous drug dispersions utilizing modified spray-drying apparatus*. Patent WO0363822A2.

Bhende S., Jadhav N., 2012. *Moringa Coagulant as a Stabilizer for Amorphous Solids: Part I*. AAPS PharmSciTech 13 (2), 400–410.

Bhatt, V., Shete, G., Bansal, A.K., 2015. *Mechanism of generation of drug nanocrystals in celecoxib: mannitol nanocrystalline solid dispersion*. Int. J. Pharm. 495 (1), 132–139.

Bhugra C., Pikal M.J., 2008. *Role of thermodynamic, molecular and kinetic factors in crystallization from the amorphous state*. J. Pharm. Sci. 97 (4), 1329–1349.

Blanco M., Castillo M., Peinado A., Beneyto R., 2007. *Determination of low analyte concentrations by near-infrared spectroscopy: effect of spectral pretreatments and estimation of multivariate detection limits*. Anal. Chim. Acta 581(2), 318–323.

Blanco M., Coello J., Iturriaga H., Maspoch S., Pagès J.,2000. *NIR calibration in non-linear systems: different PLS approaches and artificial neural networks*. Chemometr. Intell. Lab. 50(1), 75–82.

Blum, M.-M., John H., 2012. *Historical perspective and modern applications of attenuated total reflectance–Fourier transform infrared spectroscopy (ATR-FTIR)*. Drug Test. Anal. 4 (3–4), 298–302.

Brough C., Williams R.O., 2013. *Amorphous solid dispersions and nano-crystal technologies for poorly water-soluble drug delivery*. Int. J. Pharm. 453 (1), 157–166.

Buckton G., Gill H., 2007. *The importance of surface energetics of powders for drug delivery and the establishment of inverse gas chromatography*. Adv. Drug Deliv. Rev. 59, 1474–1479.

Byrn S.R., Xu W., Newman A.W., 2001. *Chemical reactivity in solid-state pharmaceuticals: formulation implications*. Adv. Drug Deliv. Rev. 48, 115–136.

Carson J.F., Waisbrot S.W., Jones F.T., 1943. *New form of crystalline xylitol*. J. Am. Chem. Soc. 65 (9), 1777–1778.

Çelikbilek, M., Ersundu, A.E., Aydın, S., 2012. *Crystallization kinetics of amorphous materials*. In: Yitzhak Mastai (Ed.), Advances in Crystallization Processes, 127–162.

Chaix E., Guillaume C., Guillard V., 2014. *Oxygen and Carbon Dioxide Solubility and Diffusivity in Solid Food Matrices: A Review of Past and Current Knowledge*. Compr. Rev. Food Sci. F. 13, 261–286.

Chavan R.B., Thipparaboina R., Kumar D., Shastri N.R., 2016. *Co amorphous systems: A product development perspective*. Int. J. Pharm. 515, 403–415.

Chen X., Morris K.R., Griesser U.J., Byrn S.R., Stowell J.G., 2002. *Reactivity differences of indomethacin solid forms with ammonia gas*, J. Am. Chem. Soc. 124, 15012–15019.

Chieng N., Rades T., Aaltonen J., 2011. *An overview of recent studies on the analysis of molecular pharmaceutical polymorphs*. J. Pharm. Biomed. Anal. 55 (4), 618–644.

Clas S.-D., Dalton C.R., Bruno C.Hancock B.C., 1999. *Differential scanning calorimetry: applications in drug development*. Pharm. Sci. Technol. To. 2 (8), 311–320.

Cooper E.R., 2010. *Nanoparticles: A personal experience for formulating poorly water soluble drugs*. J. Control. Release 141, 300–302.

Colthup, N., Daly, L., Wiberley, S., 1990. *Introduction to infrared and Raman spectroscopy*. 3rd ed., Academic Press, Inc., San Diego.

Craig D.Q.M., Royall P.G., Kett V.L., Hopton M.L., 1999. *The relevance of the amorphous state to pharmaceutical dosage forms: glassy drugs and freeze dried systems*. Int. J. Pharm. 179, 179–207.

Crupi V., Ficarra R., Guardo M., Majolino D., Stancanelli R., Venuti V., 2007. *UV-vis and FTIR-ATR spectroscopic techniques to study the inclusion complexes of genistein with β-cyclodextrins*. J. Pharm. Biomed. Anal. 44(1), 110–117.

Cui Y., 2007. *A material science perspective of pharmaceutical solids*. Int. J. Pharm. 339, 3–18.

Davidson P., Sun W.Q., 2001. *Effect of Sucrose/Raffinose Mass Ratios on the Stability of Co-Lyophilized Protein During Storage Above the T_g*. Pharm. Res. 18 (4), 474–479.

DeCrosta M.T., Schwartz J.B., Wigent R.J., Marshall K., 2001. *Thermodynamic analysis of compact formation; compaction, unloading, and ejection II. Mechanical energy (work) and thermal energy (heat) determinations of compact unloading and ejection*. Int. J. Pharm. 213, 45–62.

de Veij M., Vandenabeele P., De Beer T., Remon J.P., Moens L., 2009. *Reference database of Raman spectra of pharmaceutical excipients*. J. Raman Spectrosc. 40, 297–307.

Di Martino P., Conflant P., Drache M., Huvenne J.-P., Guyot-Hermann A.-M., 1997. *Preparation and physical characterization of form II and III paracetamol*, J. Therm. Anal. 48, 447–458.

Di Martino P., Guyot-Hermann A.-M., Conflant P., Drache M., Guyot J.-C., 1996. *A new pure paracetamol for direct compression: the orthorhombic form*, Int. J. Pharm. 128, 1–8.

Di Martino P., Palmieri G.F., Martelli S., 2000. *Molecular mobility of the paracetamol amorphous form*. Chem. Pharmaceut. Bull. 48 (8), 1105–1108.

Diogo, H.P., Pinto, S.S., Moura Ramos, J.J., 2007. *Slow molecular mobility in the crystalline and amorphous solid states of pentitols: a study by thermally stimulated depolarisation currents and by differential scanning calorimetry*. Carbohydr. Res. 342, 961–969.

Dixon, P.G., Ahvenainen, P., Aijazi, A.N., Chen, S.H., Lin, S., Augusciak, P.K., Borrega, M., Svedström, K., Gibson, L.J., 2015. *Comparison of the structure and flexural properties of Moso, guadua and Tre Gai bamboo*. Constr. Build. Mater. 90, 11–17.

Dong Y.-D., Ben J. Boyd B.J., 2011. *Applications of X-ray scattering in pharmaceutical science*. Int. J. Pharm. 417, 101–111.

Dudognon E., Danède F.,1 Descamps M., Correia N.T., 2008. *Evidence for a New Crystalline Phase of Racemic Ibuprofen*. Pharm. Res., 25 (12), 2853–2858.

Ediger M.D., 2000. *Spatially heterogeneous dynamics in supercooled liquids*, Annu. Rev. Phys. Chem. 51, 99–128.

Ediger M., Angell C., Nagel S., 1996. *Supercooled liquids and glasses*. J. Phys. Chem. 100 (31), 13200–13212.

Faber, N.M. 1999. *Multivariate sensitivity for the interpretation of the effect of spectral pretreatment methods on near-infrared calibration model predictions*. Anal. Chem. 71(3), 557–565.

Fearn T., 2003. *Are two pretreatments better than one?* NIR news 14(6), 9–11.

Fukuoka E., Makita M., Yamamura S., 1989. *Glassy state of pharmaceuticals. III. Thermal properties and stability of glassy pharmaceuticals and their glass systems*. Chem. Pharm. Bull. 37, 1047–1050.

Gao Y., Liao J., Qi X., Zhang J., 2013. *Coamorphous repaglinide–saccharin with enhanced dissolution*. Int. J. Pharm. 450, 290–295.

Gaydou V., Kister J., Dupuy N., 2011. *Evaluation of multiblock NIR/MIR PLS predictive models to detect adulteration of diesel/biodiesel blends by vegetal oil.* Chemometr. Intell. Lab. 106 (2), 190–197.

Giron D., 2003. *Characterisation of salts of drug substances*. J. Therm. Anal. Cal. 73, 441–457.

Giron D., Goldbronn C., 1995. *Place of DSC purity analysis in pharmaceutical development*. J. Therm. Anal. Calorim., 44 (1), 217–251.

Grace GmbH & Co., *Syloid 244 FP product information*, 2015.

Grant D.J.W., 1999. *Theory and Origin of Polymorphism in pharmaceutical solids*, in: Brittain HG (Ed.), Polymorphism in Pharmaceutical solids. Marcel Dekker. New York, USA, 1–33.

Greco K., Bogner R., 2010. *Crystallization of Amorphous Indomethacin during Dissolution: Effect of Processing and Annealing*. Mol. Pharm. 7 (5), 1406–1418.

Guillory J.K., 1999. *Generation of polymorphs, hydrates, solvates, and amorphous solids*, in: H. G. Brittain, editor Polymorphs in pharmaceutical solids: Marcel Dekker, Inc., NY, USA, 183–226.

Gunawan L., Johari G.P., Shanker R.M., 2006. *Structural relaxation of acetaminophen glass*. Pharm. Res. 23 (5), 967–979.

Guo Y., Byrn S.R., Zografi G., 2000. *Physical Characteristics and Chemical Degradation of Amorphous Quinapril Hydrochloride*, J. Pharm. Sci. 89 (1), 128–143.

Haque M.K., Kawai K., Suzuki T., 2006. *Glass transition and enthalpy relaxation of amorphous lactose glass*. Carbohyd. Res. 341, 1884–1889.

Hancock C., 2002. *Disordered drug delivery: destiny, dynamics and the deborah number*. J. Pharm. Pharmacol. 54, 737–746.

Hancock B.C. and Dalton C.R., 1999. *The Effect of Temperature on Water Vapor Sorption by Some Amorphous Pharmaceutical Sugars*. Pharm. Dev. Technol., 4 (1), 125–131.

Hancock B.C., Parks M., 2000. *What is the true solubility advantage for amorphous pharmaceutics?* Pharm. Res., 17, 397–404.

Hancock B.C., Zografi, G., 1997. *Characteristics and significance of the amorphous state in pharmaceutical systems*. J. Pharm. Sci. 86 (1), 1–12.

Hancock B.C., Zografi G., 1994. *The relationship between glass transition temperature and the water content of amorphous pharmaceutical solids*. Pharm. Res. 11 (4), 471–477.

Heljo V.P., Nordberg A., Tenho M., Virtanen T., Jouppila K., Salonen J., Maunu S.L., Juppo A.M., 2012. *The Effect of Water Plasticization on the Molecular Mobility and Crystallization Tendency of Amorphous Disaccharides*. Pharm. Res. 29, 2684–2697.

Hellrup, J., Mahlin, D., 2011. *Pharmaceutical micro-particles give amorphous sucrose higher physical stability*. Int. J. Pharm. 409 (1–2), 96–103.

Hoppu P., Jouppila K., Rantanen J., Schantz S., Juppo A.M., 2007. *Characterization of blends of paracetamol and citric acid*. J. Pharm. Pharmacol. 59, 373–381.

Horvat M., Meštrović E., Danilovski A., Craig D.Q.M., 2005. *An investigation into the thermal behaviour of a model drug mixture with amorphous trehalose*. Int. J. Pharm. 294, 1–10.

Igantious F., Sun L., 2003. *Electrospun amorphous pharmaceutical compositions*, WO2004014304A2.

Igne B., Reeves J.B., McCarty G., Hively W.D., Lund E., Hurburgh C.R. Jr, 2010. *Evaluation of spectral pretreatments, partial least squares, least squares support vector machines and locally weighted regression for quantitative spectroscopic analysis of soils*. J. Near Infrared Spec. 18 (3), 167–176.

Izutsu K., Yoshioka S., Terao T., 1993. *Decreased protein-stabilizing effects of cryoprotectants due to crystallization*. Pharm. Res. 10 (8), 1232–1237.

Jensen F., 2017. *Introduction to Computational Chemistry*, third ed., John Wiley & sons, Ltd, Aarhus, 450.

Johansson, J., Pettersson, S., Folestad, S., 2005. *Characterization of different laser irradiation methods for quantitative Raman tablet assessment*. J. Pharm. Biomed. 39, 510–516.

Kadoya S., Fujii K., Izutsu K.-i., Yonemochi E., Terada K., Yomota C., Kawanishi T., 2010. *Freeze-drying of proteins with glass-forming oligosaccharide-derived sugar alcohols*. Int. J. Pharm. 389, 107–113.

Kauffman J.F., Batykefer L.M., Tuschel D.D., 2008. *Raman detected differential scanning calorimetry of polymorphic transformations in acetaminophen*. J. Pharmaceut. Biomed. 48, 1310–1315.

Kaushal M., Gupta P., Bansal A. K., 2004. *Amorphous drug delivery systems: Molecular aspects, design, and performance*, Crit. Rev. Ther. Drug. Carrier Syst. 21, 133–193.

Kestur U.S., Taylor L.S., 2013. *Evaluation of the Crystal Growth Rate of Felodipine Polymorphs in the Presence and Absence of Additives As a Function of Temperature*. Cryst. Growth Des. 13, 4349−4354.

Kinnari, P., Mäkilä, E., Heikkilä, T., Salonen, J., Hirvonen, J., Santos, H.A., 2011. *Comparison of mesoporous silicon and non-ordered mesoporous silica materials as drug carriers for itraconazole*. Int. J. Pharm. 414 (1–2), 148–156.

Kontro, I., Wiedmer, S.K., Hynönen, U., Penttilä, P.A., Palva, A., Serimaa, R., 2014. *The structure of Lactobacillus brevis surface layer reassembled on liposomes differs from native structure as revealed by SAXS*. Biochim. Biophys. Acta 1838 (8), 2099–2104.

Lai M.C., Topp E.M., 1999. *Solid-state chemical stability of proteins and peptides*. J. Pharm. Sci. 88, 489–500.

Laitinen, R., Löbmann, K., Strachan, C.J., Grohganz, H., Rades, T., 2013. *Emerging trends in the stabilization of amorphous drugs*. Int. J. Pharm. 453, 65–79.

Larkin P. J., 2011. *General outline and strategies for IR and Raman spectral interpretation*. In IR and Raman Spectroscopy: Principles and Spectral Interpretation 1st ed., 117–134.

Lehmkemper K., Kyeremateng S.O., Heinzerling O., Degenhardt M., Sadowski G., 2017. *Impact of polymer type and relative humidity on the long-term physical stability of amorphous solid dispersions*. Mol. Pharm. 14, 4374–4386.

Li Y., Han J., Zhang G.G.Z., Grant D.J.W., Suryanarayanan R., 2000. *In situ dehydration of carbamazepine dihydrate: A novel technique to prepare amorphous anhydrous carbamazepine*. Pharm. Dev. Tech. 5, 257–266.

Limnell T., Santos H.A., Mäkilä E., Heikkilä T., Salonen J., Murzin D.Y., Kumar N., Laaksonen T., Peltonen L., Hirvonen J., 2011. *Drug Delivery Formulations of Ordered and Nonordered Mesoporous Silica: Comparison of Three Drug Loading Methods*. J. Pharm. Sci. 100 (8), 3294–3306.

Lipinski C., 2002. *Poor Aqueous Solubility – an Industry Wide Problem in Drug Discovery*. Am. Pharm. Rev. 5 (3), 82–85.

Lipiäinen T., Peltoniemi M., Räikkönen H., Juppo A., 2016. *Spray-dried amorphous isomalt and melibiose, two potential protein-stabilizing excipients*. Int. J. Pharm. 510, 311–322.

Lipiäinen T., Räikkönen H., Kolu A.-M., Peltoniemi M., Juppo A., 2018. *Comparison of melibiose and trehalose as stabilising excipients for spray-dried β-galactosidase formulations*. Int. J. Pharm. 543, 21–28.

Liu Y., Bhandari B., Zhou W., 2006. Glass Transition and Enthalpy Relaxation of Amorphous Food Saccharides: A Review. J. Agric. Food Chem. 54, 5701–5717.

Luthra S.A., Hodge I.M., Utz M., Pikal M.J., 2008. *Correlation of Annealing with Chemical Stability in Lyophilized Pharmaceutical Glasses*. Pharmaceutical sciences, 97 (12), 5240–5251.

Löbmann K., Laitinen R., Grohganz H., Strachan C., Rades T., Gordon K.C., 2013a. *A theoretical and spectroscopic study of co-amorphous naproxen and indomethacin*. Int. J. Pharm. 453, 80–87.

Löbmann K., Grohganz H., Laitinen R., Strachan C., Rades T., 2013b. *Amino acids as co-amorphous stabilizers for poorly water soluble drugs – Part 1: Preparation, stability and dissolution enhancement*. Eur. J. Pharm. Biopharm. 85, 873–881.

Löbmann K., Laitinen R., Strachan C., Rades T., Grohganz H., 2013c. *Amino acids as co-amorphous stabilizers for poorly water-soluble drugs – Part 2: Molecular interactions*. Eur. J. Pharm. Biopharm. 85, 882–888.

Mah P.T., Laaksonen T., Rades T., Aaltonen J., Peltonen L., Strachan C.J., 2014. *Unravelling the relationship between degree of disorder and the dissolution behavior of milled glibenclamide*. Mol. Pharm. 11 (1), 234–42.

Manca C., Martin C., Roubin P., 2003. Comparative study of gas adsorption on amorphous ice: thermodynamic and spectroscopic features of the adlayer on the surface. J. Phys. Chem. B 107, 8929–8934.

Mártha C., Jójárt-Laczkovich O., Szabó-Révész P., 2014. *Effect of co-grinding on crystallinity of clopidogrel bisulfate*. Chem. Eng. Technol. 37 (8), 1393–1398.

Mazzobre M.F., Aguilera J.M., Buera M.P., 2003. *Microscopy and calorimetry as complementary techniques to analyze sugar crystallization from amorphous systems*. Carbohyd. Res. 338, 541–548.

Martínez L.M., Videa M., López-Silva G.A., de los Reyes C.A., Cruz-Angeles J., González N., 2014. *Stabilization of amorphous paracetamol based systems using traditional and novel strategies*. Int. J. Pharm 477, 294–305.

McCreery, R.L., 2000. *Raman Spectroscopy for Chemical Analysis*. John Wiley & Sons Inc., New York.

Mellaerts R., Jammaer J.A.G., Van Soeybroeck M., Chen H., Van Humbeeck J., Augustijns P., Van den Mooter G., Martens J.S., 2008. *Physical state of poorly water soluble therapeutic molecules loaded into SBA-15 ordered mesoporous silica carriers: a case study with itraconazole and ibuprofen*. Langmuir 24, 8651–8659.

Mensink, M.A., Frijlink H.W., van der Voort Maarschalk K., and Hinrichs W.L., 2017. *How sugars protect proteins in the solid state and during drying: Mechanisms of stabilization in relation to stress conditions*. Eur. J. Pharm. Biopharm. 114, 288–295.

Mensink, M.A., Nethercott M.J., Hinrichs W.L., van der Voort Maarschalk K., Frijlink H.W., Munson E.J., M.J. Pikal, 2016. *Influence of Miscibility of Protein-Sugar Lyophilizates on Their Storage Stability*. AAPS J. 18 (5), 1225–1232.

Merisko-Liversidge E., Liversidge G.G., Cooper E.R., 2003. *Nanosizing: a formulation approach for poorly-water-soluble compounds*, Eur. J. Pharm. Sci. 18 (2), 113–120.

Morales J.O., Watts A.B., McConville J.T., 2012. *Mechanical Particle-Size Reduction Techniques,* in Williams R.O. III, Watts A.B., Miller D.A., Formulating Poorly Water Soluble Drugs, American Association of Pharmaceutical Scientists.

Mu H., Holm R., Müllertz A., 2013. *Lipid-based formulations for oral administration of poorly water-soluble drugs*. Int. J. Pharm. 453, 215–224.

Nanubolu B.J., Burley J.C., 2012. *Investigating the recrystallization behavior of amorphous paracetamol by variable temperature Raman studies and surface Raman mapping*. Mol. Pharm. 9, 1544–1558.

Nichols G., Frampton C.S., 1998. *Physicochemical characterization of the orthorhombic polymorph of paracetamol crystallized from solution*. J. Pharmaceut. Sci. 87 (6), 684–693.

Okamoto N., Oguni M., 1996. Discovering of crystal nucleation proceeding much below the glass transition temperature in a super cooled liquid. Solid State Commun. 99 (1), 53–56.

Palomäki E., Ehlers H., Yliruusi J., 2016. *Developing a method to assess crystallinity of xylitol using Raman spectroscopy*. Conference paper in PBP world meeting.

Patterson J. E., Michael B. J., Forster A. H., Lancaster R. W., Butler J. M., Rades T., 2005. *The influence of thermal and mechanical preparative techniques on the amorphous state of poorly soluble compounds*, J. Pharm. Sci. 94, 1998–2012.

Paudel A., Raijada D., Rantanen J., 2015. *Raman spectroscopy in pharmaceutical product design*. Adv. Drug Deliv. Rev. 89, 3–20.

Pelletier M.J., 2003. *Quantitative analysis using Raman spectroscopy*. Appl. Spectrosc. 57, 20A–42A.

Pellow-Jarman M.V., Hendra P.J., Lehnert R.J., 1996. *The dependence of Raman signal intensity on particle size for crystal powders*. Vib. Spectrosc. 12, 257–261.

Perrin M.A., Neumann M.A., Elmaleha H., Zaske L., 2009. *Crystal structure determination of the elusive paracetamol Form III*. Chem. Commun., 3181–3183.

Pessi J, Lassila I, Meriläinen A, Räikkönen H, Hæggström E, Yliruusi J. 2016. Controlled Expansion of Supercritical Solution: A Robust Method to Produce Pure Drug Nanoparticles with Narrow Size-Distribution. J Pharm Sci. 105(8), 2293–7.

Priemel, P.A., Grohganz, H., Gordon, K.C., Rades, T., Strachan, C.J., 2012. *The impact of surface- and nano-crystallisation on the detected amorphous content and the dissolution behavior of amorphous indomethacin*. Eur. J. Pharm. Biopharm. 82, 187–193.

Qi S., Avalle P., Saklatvala R., Craig D.Q.M., 2006. *An investigation into the effects of thermal history on the crystallisation behaviour of amorphous paracetamol*. Eur. J. Pharm. Biopharm. 69, 364–371.

Riikonen, J., Mäkilä, E., Salonen, J., Lehto, V.-P., 2009. *Determination of the physical state of drug molecules in mesoporous silicon with different surface chemistries*. Langmuir 25 (11), 6137–6142.

Rinnan Å., van der Berg F., Engelsen S.B., 2009. *Review of the most common pre-processing techniques for near-infrared spectra*. Trends Anal. Chem. 28 (10), 1201–1222.

Roberts C.J., Debenedetti P.G., 2002. *Engineering pharmaceutical stability with amorphous solids*, AIChE Journal 48, 1140–1144.

Roos Y., 1993. *Melting and glass transitions of low molecular weight carbohydrates*. Carbohyd. Res., 238, 39–48.

Ruecroft G., Hipkiss D., Ly T., Maxted N., Cains P.W., 2005. *Sonocrystallization: The use of ultrasound for improved industrial crystallization*. Org. Process Res. Dev. 9, 923–932.

Sandhu H., Shah N., Chokshi H., Malick A.W., 2014. *Overview of Amorphous Solid Dispersion Technologies*. In Amorphous Solid Dispersions - Theory and Practice. Ed. Shah N., Chokshi H, Sandhu H., Malick A.W., Choi D.S., Springer. New York, USA.

Sauer D., Cerea M., DiNunzio J., McGinity J., 2013. *Dry powder coating of pharmaceuticals: A review*. Int. J. Pharm. 457, 488–502.

Savolainen M., 2008. *New Insights into the Amorphous State and Related Solid-State Transformations*. Academic dissertation, University of Helsinki.

Schebor C., Mazzobre M.F., del Pilar Buera M., 2010. *Glass transition and time-dependent crystallization behavior of dehydration bioprotectant sugars*. Carbohyd. Res. 345, 303–308.

Semjonov K., Kogermann K., Laidmäe I., Antikainen O., Strachan C.J., Ehlers H., Yliruusi J., Heinämäki J., 2017. *The formation and physical stability of two-phase solid dispersion systems of indomethacin in supercooled molten mixtures with different matrix formers*. Eur. J. Pharm. Sci. 97, 237–246.

Semjonov K., Salm M., Lipiäinen T., Kogermann K., Lust A., Laidmäe I., Antikainen O., Strachan C.J., Ehlers H., Yliruusi J., Heinämäki J., 2018. *Interdependence of particle properties and bulk powder behavior of indomethacin in quench-cooled molten two-phase solid dispersions*. Int. J. Pharm. 541, 188–197.

Serajuddin, A.T., 1999. Solid dispersion of poorly water-soluble drugs: early promises, subsequent problems, and recent breakthroughs. J. Pharm. Sci., 88, 1058–1066.

Sillescu H., 1999. *Heterogeneity at the glass transition: a review*. J. Non-Cryst. Solids 243, 81–108.

Slade L., Levine H., 1991. Beyond water activity – recent advances based on an alternative approach to the assessment of food quality and safety. Crit. Rev. Food Sci., 30 (2–3), 115–360.

Smith T.J., Gauzer G., 2003. High pressure compaction for pharmaceutical formulations. WO2004058222A1.

Sprockel L., Sen M., Shivanand P., Prapaitrakul W., 1997. *A melt-extrusion process for manufacturing matrix drug delivery systems*. Int. J. Pharm. 155, 191–199.

Strachan C.J., Rades T., Gorden K., Rantanen J., 2007. *Raman spectroscopy for quantitative analysis of pharmaceutical solids*. J. Pharm. Pharmacol. 59, 179–192.

Stuart B., 2000. *Infrared spectroscopy*. Kirk-Othmer Encyclopedia of Chemical Technology, 1–18.

Surana R., Pyne A., Suryanarayanan R., 2004. *Effect of Preparation Method on Physical Properties of Amorphous Trehalose*. Pharm. Res. 21 (7), 1167–1176.

Surwase S.A., Boetker J.P., Saville D., Boyd B.J., Gordon K.C., Peltonen L., Strachan C.J., 2013. *Indomethacin: New Polymorphs of an Old Drug*. Mol. Pharm. 10, 4472–4480.

Surwase, S.A., Itkonen, L., Aaltonen, J., Saville, D., Rades, T., Peltonen, L., et al., 2015. *Polymer incorporation method affects the physical stability of amorphous in- domethacin in aqueous suspension*. Eur. J. Pharm. Biopharm. 96, 32–43.

Suslick K. S., Price G. J., 1999. *Applications of ultrasound to materials chemistry*, Annu. Rev. Mater. Sci. 29, 295–326.

Sussich F., Urbani R., Princivalle F., Cesàro A., 1998. *Polymorphic Amorphous and Crystalline Forms of Trehalose*. J. Am. Chem. Soc. 120, 7893–7899.

Swallen S.F., Kearns K.L., Mapes M.K., Kim Y.S., McMahon R.J., Ediger M.D., Wu T., Yu L., Satija S., 2007. *Organic glasses with exceptional thermodynamic and kinetic stability*. Science 315, 353–356.

Szoke S., Szabo C., Gyuricza L., Singer C., Niddam-Hildesheim V., Sterimbaum G., 2005. *Process for preparation of amorphous form of a drug*. WO2005/117837A1.

Takeuchi H., Nagira S., Yamamoto H., Kawashima Y., 2005. *Solid dispersion particles of amorphous indomethacin with fine porous silica particles by using spray–drying method*. Int. J. Pharm. 293, 155–164.

Talja, R.A., Roos, Y.H., 2001. *Phase and state transition effects on dielectric, mechanical, and thermal properties of polyols*. Thermochim. Acta 380, 109–121.

Tian, F., Zhang, F., Sandler, N., Gordon, K.C., McGoverin, C.M., Strachan, C.J., Saville, D.J., Rades, T., 2007. Influence of sample characteristics on quantification of carbamazepine hydrage formation by X-ray powder diffraction and Raman spectroscopy. Eur. J. Pharm. Biopharm. 66, 466–474.

Tonnis, W.F., Mensink M.A., de Jager A., van der Voort Maarschalk K., Frijlink H.W., Hinrichs W.L., 2015. *Size and molecular flexibility of sugars determine the storage stability of freeze-dried proteins*. Mol. Pharm. 12 (3), 684–94.

Trasi N.J., Taylor L.S., 2012. *Effect of polymers on nucleation and crystal growth of amorphous acetaminophen*. Cryst. Eng. Comm. 14, 5188–5197.

Tripathi, P., Romanini, M., Tamarit, J.L., Macovez, R., 2015. *Collective relaxation dynamics and crystallization kinetics of the amorphous Biclotymol antiseptic*. Int. J. Pharm. 495 (1), 420–427.

Ueda, H., Ida, Y., Kadota, K., Tozuka, Y., 2014. *Raman mapping for kinetic analysis of crystallization of amorphous drug based on distributional images*. Int. J. Pharm. 462, 115–122.

Vaka S.R.K., Bommana M.M., Desai D., Djordjevic J., Phuapradit W., Shah N., 2014. *Excipients for Amorphous Solid Dispersions*. In Amorphous Solid Dispersions Theory and Practice, Ed. Shah N., Sandhu H., Choi D.S., Chokshi H., A. Waseem Malick A.W., USA, 123–164.

Vanarase A.U., Alcalà M., Rozo J.I.J., Muzzio F.J., Romanãch R.J., 2010. *Real-time monitoring of drug concentration in a continuous powder mixing process using NIR spectroscopy*. Chem. Eng. Sci. 65 (21), 5728–5733.

Van Dooren A.A., Müller B.W., 1984. *Purity determinations of drugs with differential scanning calorimetry (DSC) – a critical review*. Int. J. Pharm. 20, 217–233.

Vasconcelos, T., Sarmento B., Costa, P., 2007. *Solid dispersions as strategy to improve oral bioavailability of poor water soluble drugs*. Drug Discov. Today, 12, 1068–1075.

Viel Q., Brandel C., Coquerel G., Petit S., 2017. *Crystallization from the Amorphous State of a Pharmaceutical Compound: Impact of Chirality and Chemical Purity*. Cryst. Growth Des. 2017, 17, 337–346.

Wang W., 2000. *Lyophilization and development of solid protein pharmaceuticals*. Int. J. Pharm. 203, 1–60.

Watanabe T., Wakiyama N., Usui F., Ikeda M., Isobe T., Senna M., 2001. *Stability of amorphous indomethacin compounded with silica*. Int. J. Pharm. 226, 81–91.

Weinhold S., Litt M., Lando J.B., 1984. The effect of crystallite on the electric field induced to crystals phase transition in poly(vinylodene fluoride). Ferroelectrics 57, 277–296.

Willart J.F., Dudognon E., Mahieu A., Eddleston M., Jones W., Descamps M., 2017. *The Role of Cracks in the Crystal Nucleation Process of Amorphous Griseofulvin*. Eur. Phys. J. Spec. Top. 226 (5), 837–847.

Wolfrom M.L., Kohn E.J., 1942. *Crystalline Xylitol*. J. Amer. Chem. Soc. 64, 1739.

Wu T., Yu L., 2006. *Surface crystallization of indomethacin below T_g*. Pharm. Res. 23 (10), 2350–2355.

Wu T., Sun Y., de Villiers M.M., Yu L., 2007. *Inhibiting surface crystallization of amorphous indomethacin by nanocoating*. Langmuir 23, 5148–5153.

Xu W., Riikonen J., Lehto V.-P., 2013. *Mesoporous systems for poorly soluble drugs*. Int. J. Pharm. 453, 181–197.

Ye X., Wai C.M.,2003. *Making nanomaterials in supercritical fluids: a review*. J. Chem Educ. 80(2), 198–204.

Yu L., 2001. Amorphous pharmaceutical solids: preparation: characterization and stabilization. Adv. Drug Deliv. Rev. 28, 27–42.

Yu L., 2016. Surface mobility of molecular glasses and its importance in physical stability. Adv. Drug. Deliv. Rev. 100, 3–9.

Yu Z., Johnston K.P., Williams R.O., 2006. Spray freezing into liquid versus spray- freeze drying: Influence of atomization on protein aggregation and biological activity. Eur. J. Pharm. Sci. 27, 9–18.

Yu L., Mishra D.S., Rigsbee D.R., 1998. Determination of the glass properties of D-mannitol using sorbitol as an impurity. J. Pharm. Sci. 87, 774–777.

Zografi G., Newman A., 2017. Interrelationships between structure and the properties of amorphous solids of pharmaceutical interest. J. Pharm. Sci. 106, 5–27.

Zhou, X., Hines P., Borer M.W., 1998. Moisture determination in hygroscopic drug substances by near infrared spectroscopy. J. Pharm. Biomed. 17 (2), 219–225.

Zhu L., Wong L., Yu L., 2008. *Surface-Enhanced crystallization of amorphous nifedipine*. Mol. Pharm. 5 (6), 921–926.

ISBN 978-951-51-6410-0 (PRINT)
ISBN 978-951-51-6411-7 (ONLINE)
ISSN 2342-3161 (PRINT)
ISSN 2342-317X (ONLINE)
http://ethesis.helsinki.fi

HELSINKI 2020